NATIONAL ADVISORY COMMITTEE FOR AERONAUTICS

TECHNICAL NOTE 4306

TEMPERATURE AND THERMAL-STRESS DISTRIBUTIONS IN SOME STRUCTURAL ELEMENTS HEATED AT A CONSTANT RATE

By William A. Brooks, Jr.

Langley Aeronautical Laboratory
Langley Field, Va.

Washington
August 1958

NATIONAL ADVISORY COMMITTEE FOR AERONAUTI

TECHNICAL NOTE 4306

TEMPERATURE AND THERMAL-STRESS DISTRIBUTIONS IN SOME STRUCTURAL ELEMENTS HEATED AT A CONSTANT RATE

By William A. Brooks, Jr.

SUMMARY

Analytical solutions are given for the temperature and thermal-stress distributions in thick skins and structural elements such as angle, channel, T-, and H-sections when heated at a constant rate. Certain of the analytical solutions are evaluated for selected cross-sectional proportions. The results are presented in the form of charts involving dimensionless temperature, stress, and time parameters and therefore are applicable for different materials and heating rates and absolute size of the section. The results have been found useful for analyzing and correlating experimental data.

INTRODUCTION

Interest in the behavior of structural elements exposed to the heating rates and elevated temperatures of high-speed flight has resulted in a great deal of research, both theoretical and experimental, on the effects of aerodynamic heating. The variable nature of the heat flux encountered in a typical flight plan complicates the problem greatly. By considering constant heating rates, it is possible to simplify both theoretical and experimental aspects of the problem and still obtain valuable information concerning the primary effects of aerodynamic heating.

The present paper contains one-dimensional solutions for temperature and stress distributions in thick skins and structural elements such as angle, channel, T-, and H-sections when heated at a constant rate. These solutions have been found to be useful for analyzing and correlating experimental data. (See ref. 1.) Although some of the solutions have been published previously (for example, refs. 2 to 4), they are derived herein in order to make the presentation complete.

Certain of the analytical expressions are evaluated for selected section proportions. The results are presented in the form of charts involving dimensionless temperature, stress, and time parameters and therefore are applicable for different materials and absolute size of the sections.

SYMBOLS

a,b,c	constants
A,B,C	constants
c	specific heat, Btu/lb-°F
E	modulus of elasticity, psi
k	thermal conductivity, Btu/ft-sec-°F
l	length of leg of angle, ft
n	integer
q	heating rate, Btu/ft^2-sec
t	thickness, ft
T	temperature, °F
ΔT	maximum temperature difference, °F
w	specific weight, lb/cu ft
x,y	coordinates
α	thermal coefficient of expansion, in./in-°F
β_n	root of characteristic equation
ϵ	strain, in./in.
ζ,η	dimensionless space coordinates
ζ_i	dimensionless length, l_i/t_2
θ	dimensionless time parameter, $k\tau/cwt^2$
μ	Poisson's ratio
σ	thermal stress, psi (positive for tension)
τ	time, sec

ϕ	dimensionless temperature parameter, $\left(T - T_o\right)\dfrac{k}{qt}$

Subscripts:

j	junction of elements
o	initial
1	element 1
2	element 2
av	average
max	maximum
min	minimum
i	integer

TEMPERATURE DISTRIBUTION

In the following sections, temperature distributions obtained by assuming constant material properties and making exact solutions of the one-dimensional heat-conduction equation are presented. First, the simple case of a skin, thin in the thermal sense, is discussed in order to introduce some of the dimensionless parameters which are used in the present paper. Then the solutions for thermally thick skins are given and the thin skin is examined as a special case of the thick skin. Finally, the one-dimensional temperature distribution in some common structural shapes is given.

Thin Skin

If it is assumed that a skin is heated on one side, that there is no variation of temperature through the thickness or in the plane of the skin, and that there is no transfer of heat through the unheated face by means of convection or radiation, the differential equation governing the temperature of the skin can be obtained by equating the rate at which the skin absorbs heat to the rate at which heat is provided, or

$$cwt \frac{dT}{d\tau} = q \tag{1}$$

Integration yields

$$T - T_0 = \frac{1}{cwt} \int_0^\tau q \, d\tau$$

or

$$T - T_0 = \frac{q_{av}\tau}{cwt} \tag{2}$$

where

$$q_{av} = \frac{1}{\tau} \int_0^\tau q \, d\tau$$

In a convenient dimensionless form, equation (2) becomes, for a constant heating rate,

$$\phi = \theta \tag{3}$$

where

$$\phi = (T - T_0)\frac{k}{qt}$$

$$\theta = \frac{k\tau}{cwt^2}$$

The principal limitation of equation (3) is that the variation in temperature through the thickness must be negligible; or, in the thermal sense, that the skin be thin. Although this solution is called the "thin-skin" solution, the actual thickness does not necessarily have to be small. A thin skin can best be defined by considering it as a special case of a thick plate as is done in the next section.

A frequent use is made of equation (1) or (2) in the calibration of the heating rate produced at a given point by a heater arrangement. The calibration is accomplished by placing a thin skin before the heater and, with the heater in operation, recording temperature rise as a function of time. Once the rate of temperature rise has been determined, the heating rate may be calculated by using equation (1) if the pertinent material properties are known.

Figure 1 shows the relation between the heating rate and the rate of temperature rise calculated by equation (1) for some of the more common materials. A nomograph of equation (1), presented in figure 2, affords a rapid graphical solution of the equation and is applicable for more materials than figure 1. The typical material properties employed in deriving figure 1 and used in figure 2 are given in table I.

Thick Skin

If a thick plate, shown schematically in figure 3, is subjected to a constant heating rate on one face, experiences temperature variation through the thickness only, and experiences no heat transfer at the unheated face, the temperature distribution (derived in appendix A and ref. 2) is given by

$$\phi = \theta + \frac{\eta^2}{2} - \frac{1}{6} - \frac{2}{\pi^2}\sum_{n=1}^{\infty}(-1)^n \frac{\cos n\pi\eta}{n^2} e^{-n^2\pi^2\theta} \qquad (4a)$$

where

$$\phi = (T - T_o)\frac{k}{qt}$$

$$\theta = \frac{k\tau}{cwt^2}$$

$$\eta = \frac{y}{t}$$

From equation (4a), temperature distributions have been calculated for a thick skin of any material and thickness subjected to a constant heating rate. These temperature distributions are plotted in figure 4 .

as a function of time for given locations through the thickness and in figure 5 as a function of location at given times. At large values of the time parameter $\theta (\theta > 0.4)$, the series term in equation (4a) contributes a negligible amount to the temperature parameter, which then becomes a linear function of time. The temperature-rise rate becomes constant for any location through the thickness, and the spacewise temperature gradient is independent of time. The result, which can be seen in figure 4, is that the temperature distribution becomes fixed, with the temperature level of the entire slab increasing uniformly. The temperature-rise rate at large values of time can also be calculated by considering only the mass and heat capacity of the skin and the heat input.

The boundary conditions of the present problem, namely, constant heat input and no loss of heat, preclude the existence of an equilibrium condition although a quasi-steady state does exist after an initial transient period. The term quasi-steady state is employed herein to describe that state in which the temperature-rise rate is constant at all points through the thickness of the slab and is hereinafter referred to as steady state. In an actual case there are heat losses through both the heated and the unheated faces, provided the unheated face does not lie in a plane of symmetry or is not insulated, and an equilibrium state does exist. The present solution must therefore be considered as an approximation for actual cases in which the temperature levels are such that excessive heat losses are not involved.

One disadvantage of equation (4a) is that it converges slowly at small values of θ. An alternate solution which can be obtained in the form of tabulated functions is given by the following equation:

$$\phi = \sum_{n=1,3,5}^{\infty} \left(2\sqrt{\frac{\theta}{\pi}} \left\{ \exp\left[-\frac{(n-\eta)^2}{4\theta} \right] + \exp\left[-\frac{(n+\eta)^2}{4\theta} \right] \right\} - \left[(n-\eta)\operatorname{erfc}\left(\frac{n-\eta}{2\sqrt{\theta}} \right) + (n+\eta)\operatorname{erfc}\left(\frac{n+\eta}{2\sqrt{\theta}} \right) \right] \right) \tag{4b}$$

At small values of θ, the first term of the series suffices. However, as θ becomes larger, more terms are necessary. Although there may be some advantage to using equation (4b) for computing temperatures, particularly at small values of θ, equation (4a) is more amenable to integration and is used to calculate the stresses.

The average temperature is found by integrating the dimensionless temperature parameter of equation (4a) over the dimensionless thickness and the result is

$$\phi_{av} = \theta$$

which is the thin-skin solution (eq. 3). This result is rather obvious inasmuch as there are no heat losses and, therefore, all available heat is employed in raising the temperature of the mass. If the heating rate is constant, then the rate of change of the average temperature must also be constant. In figure 4, the average temperature is shown as a function of time by the dashed line. In figure 5, the spacewise location of the point at which the temperature is equal to the average temperature is shown by the dashed line. The point at which the temperature is equal to the average temperature always occurs in the range $\frac{1}{\sqrt{3}} \leq \eta \leq 1$, this point being at $\eta = \frac{1}{\sqrt{3}}$ for the steady state, at which time the temperature is a parabolic function of η.

The maximum difference in the values of ϕ for the outer and inner surfaces can be obtained from equation (4a) and is

$$\Delta\phi = \frac{1}{2} \tag{5}$$

From equation (5) the maximum temperature difference is found to be

$$\Delta T = \frac{1}{2}\frac{qt}{k} \tag{6}$$

The maximum temperature difference is plotted in figure 6 as a function of qt for several materials with properties given in table I. For a given heating rate and skin thickness, the temperature difference varies inversely as the thermal conductivity; that is, materials with the larger values of thermal conductivity are associated with the smaller temperature gradients. A nomograph of equation (6), presented in figure 7, permits a rapid graphical determination of the maximum temperature difference between the heated outer surface and the insulated inner surface of the plate.

Another interesting feature of equation (4a) is the time required to obtain the maximum temperature difference. Actually, as an examination of the series term of equation (4a) will show, the maximum temperature difference is reached at an infinite time. Practically, however, it can be assumed that the steady state is reached when the series term contributes only a small amount to the solution; for example, 2 percent of the maximum temperature difference. In figure 8, the time required to produce 98 percent of the maximum temperature difference is plotted against the skin thickness. The curves for the different materials are parallel straight lines whose intercepts on the time axis vary inversely as the diffusivity k/cw. Thus, for a given thickness, the materials with the greatest diffusivity require the shortest time to reach the condition at which the maximum temperature difference exists.

One method of defining a thin skin is to set an arbitrary limit on the amount of temperature variation that can be tolerated. With this method of defining a thin skin, curves such as those shown in figure 9 can be prepared. In this figure steady-state temperature differences through the thickness are given as percentages of the heated-surface temperatures. The solid lines represent the difference between the temperatures of the heated face and the insulated face. Any combination of heated-face temperature $T_{\eta=1}$ and qt/k that lies on or above the line for the tolerable amount of variation represents a thin-skin solution. For example, assume that the temperature of the heated face is 1,000° F and that the tolerable amount of temperature difference between the two faces is arbitrarily chosen as 50° F or 5 percent. So long as the value of qt/k for the skin under consideration is equal to or less than 100, a thin-skin solution will suffice.

Angle, Channel, T-, and H-Sections

Consider next an element that is a simplified version of integral construction (fig. 10(a)) which may be regarded as part of a skin-stringer or skin-web combination. The idealization employed in the present analysis is shown in figure 10(b). All lateral surfaces except that being heated are considered to be insulated. Several such elements subjected to heating as indicated may be combined to form the sections shown in figure 11.

It is assumed that there is no temperature variation through the thicknesses t_1 and t_2 and that there is no heat loss through the unheated faces. Because of the discontinuity in the thickness and heating, it is convenient to consider the section as two elements as shown in figure 10(b), the element exposed to the heat flux q being considered as element 2. The following expressions (derived in appendix A) give the temperature distributions in the two elements:

$$\phi_1 = \frac{t_2}{t_1}\left[\frac{\theta}{\frac{\zeta_1}{\zeta_2} + \frac{t_2}{t_1}} + \frac{\frac{1}{2}\zeta^2}{\frac{\zeta_1}{\zeta_2} + \frac{t_2}{t_1}} - \frac{\frac{1}{6}\frac{\zeta_1}{\zeta_2}\left(\zeta_1^2 + 2\zeta_2^2\right) + \frac{1}{2}\zeta_1^2\frac{t_2}{t_1}}{\left(\frac{\zeta_1}{\zeta_2} + \frac{t_2}{t_1}\right)^2} - \frac{2}{\zeta_2}\sum_{n=1}^{\infty}\frac{\frac{e^{-\beta_n^2\theta}}{\beta_n^3}}{\left(\frac{\zeta_1}{\zeta_2} + \frac{t_2}{t_1}\right)\cot\beta_n\zeta_2 - \left(1 + \frac{\zeta_1}{\zeta_2}\frac{t_2}{t_1}\right)\tan\beta_n\zeta_1}\frac{\cos\beta_n\zeta}{\cos\beta_n\zeta_1}\right] \tag{7a}$$

$$\phi_2 = \frac{t_2}{t_1}\left[\frac{\theta}{\frac{\zeta_1}{\zeta_2} + \frac{t_2}{t_1}} - \frac{\frac{1}{2}\frac{\zeta_1}{\zeta_2}\frac{t_1}{t_2}\eta^2}{\frac{\zeta_1}{\zeta_2} + \frac{t_2}{t_1}} + \frac{\frac{1}{6}\frac{\zeta_1}{\zeta_2}\left(\zeta_2^2 + 2\zeta_1^2\right) + \frac{1}{2}\zeta_1^2\frac{t_1}{t_2}}{\left(\frac{\zeta_1}{\zeta_2} + \frac{t_2}{t_1}\right)^2} + \frac{t_1}{t_2}\frac{2}{\zeta_2}\sum_{n=1}^{\infty}\frac{\frac{e^{-\beta_n^2\theta}}{\beta_n^3}}{\left(\frac{\zeta_1}{\zeta_2} + \frac{t_2}{t_1}\right)\cot\beta_n\zeta_1 - \left(1 + \frac{\zeta_1}{\zeta_2}\frac{t_2}{t_1}\right)\tan\beta_n\zeta_2}\frac{\cos\beta_n\eta}{\cos\beta_n\zeta_2}\right] \tag{7b}$$

where

$$\phi_i = (T_i - T_o)\frac{k}{qt_2}$$

$$\zeta = \frac{y}{t_2} \qquad \eta = \frac{x}{t_2}$$

$$\zeta_1 = \frac{l_1}{t_2} \qquad \zeta_2 = \frac{l_2}{t_2}$$

In equations (7) the terms β_n are roots of the following transcendental equation:

$$\sin \beta_n\zeta_1 \cos \beta_n\zeta_2 + \frac{t_2}{t_1} \sin \beta_n\zeta_2 \cos \beta_n\zeta_1 = 0 \tag{8}$$

An expression for the average temperature parameter may be found by integrating equations (7a) and (7b) as follows:

$$\phi_{av} = \int_0^{\zeta_1} \phi_1 \, d\zeta + \frac{t_2}{t_1} \int_0^{\zeta_2} \phi_2 \, d\eta \tag{9}$$

Upon performing the indicated integration, the following equation is obtained:

$$\phi_{av} = \frac{\frac{t_2}{t_1}}{\frac{\zeta_1}{\zeta_2} + \frac{t_2}{t_1}} \theta \tag{10}$$

Again, as in the case of the thick skin, the average temperature is a function of the heat capacity of the section.

The infinite series of equations (7) converge very slowly for small values of θ. In order to avoid the tedious procedure of calculating the temperature for short times from equations (7), it is possible to obtain closed-form short-time solutions in terms of tabulated functions. The following equations (derived in appendix A) are approximate short-time solutions for equations (7a) and (7b), respectively:

$$\phi_1 = \frac{1}{1 + \frac{t_1}{t_2}} \left\{ \left[\theta + \frac{(\zeta_1 - \zeta)^2}{2}\right] \operatorname{erfc}\left(\frac{\zeta_1 - \zeta}{2\sqrt{\theta}}\right) - (\zeta_1 - \zeta)\sqrt{\frac{\theta}{\pi}} \exp\left[-\frac{(\zeta_1 - \zeta)^2}{4\theta}\right] + \right.$$

$$\left. \left[\theta + \frac{(\zeta_1 + \zeta)^2}{2}\right] \operatorname{erfc}\left(\frac{\zeta_1 + \zeta_2}{2\sqrt{\theta}}\right) - (\zeta_1 + \zeta)\sqrt{\frac{\theta}{\pi}} \exp\left[-\frac{(\zeta_1 + \zeta)^2}{4\theta}\right] \right\} \tag{11a}$$

$$\phi_2 = \theta - \frac{1}{1 + \frac{t_2}{t_1}}\left\{\left[\theta + \frac{(\zeta_2 - \eta)^2}{2}\right]\operatorname{erfc}\left(\frac{\zeta_2 - \eta}{2\sqrt{\theta}}\right) - \right.$$

$$(\zeta_2 - \eta)\sqrt{\frac{\theta}{\pi}}\exp\left[-\frac{(\zeta_2 - \eta)^2}{4\theta}\right] + \left[\theta + \frac{(\zeta_2 + \eta)^2}{2}\right]\operatorname{erfc}\left(\frac{\zeta_2 + \eta}{2\sqrt{\theta}}\right) -$$

$$\left.(\zeta_2 + \eta)\sqrt{\frac{\theta}{\pi}}\exp\left[-\frac{(\zeta_2 + \eta)^2}{4\theta}\right]\right\} \tag{11b}$$

Although these short-time equations give good approximations to the maximum and minimum temperatures, they do not satisfy continuity at the junction of the two elements. For short-time solutions a satisfactory approximation for the temperature at the junction is

$$\phi_j = \frac{\phi_1\Big|_{\zeta=\zeta_1} + \phi_2\Big|_{\eta=\zeta_2}}{2} \tag{12}$$

Of course, for long times the series terms in equations (7) become negligible and a quasi-steady state is reached in which the temperature is a linear function of the time parameter. The slope of the linear relation between the time and temperature parameters is, at steady state, determined by the heat capacity of the section. The existence of a state of equilibrium is precluded by the initial assumptions as was the case for the thick plate.

The maximum temperature (at $\eta = 0$), the minimum temperature (at $\zeta = 0$), and the temperature at the junction of the two elements (at $\zeta = \zeta_1$, $\eta = \zeta_2$) have been calculated for twenty-seven cases (all possible combinations of $\frac{t_2}{t_1} = 1$, 2, and 4; $\zeta_1 = 5$, 10, and 20; and

$\zeta_2 = 10$, 20, and 30). In figure 12 the maximum temperature is plotted as a dimensionless temperature parameter $\phi_{2,max}$ against the dimensionless time parameter θ, each part of the figure being for a different thickness ratio t_2/t_1. In figure 12 a straight line with slope of 1 is identified as $\zeta_1 = 0$. This line is the same as the "thin-skin" solution and serves as the upper limit for the maximum temperature by representing the case in which the maximum temperature of the heated element is not influenced by the presence of the unheated element. This line can also be represented as $\zeta_2 = \infty$, but in either case, $\zeta_1 = 0$ or $\zeta_2 = \infty$, the thickness t_2 cannot be zero or large enough to violate the assumption that there is no gradient through the thickness t_2. If ζ_2 is sufficiently large, say of the order of 50, the maximum temperature of the angle section is only slightly affected by the presence of the unheated leg.

In figure 13 the temperature at the junction of the two elements is plotted as a dimensionless parameter ϕ_j against the time parameter θ. If $l_1 = l_2$, the temperature parameter ϕ_j is a linear function of θ given by the following relation:

$$\phi_j = \frac{1}{1 + \frac{t_1}{t_2}}\theta \tag{13}$$

which is a special case of the average temperature parameter

$$\phi_{av} = \frac{\frac{t_2}{t_1}}{\frac{\zeta_1}{\zeta_2} + \frac{t_2}{t_1}}\theta \tag{14}$$

For those cases in which $\frac{l_2}{l_1} > 1$, the lower limit is the straight line defined by equation (13). For those cases where $\frac{l_2}{l_1} < 1$, the upper limit is the line defined by equation (13).

In figure 14 the minimum temperature is plotted as a dimensionless temperature parameter against the time parameter θ. The upper limit is the thin-skin solution which corresponds to $l_1 = 0$, or $\zeta_1 = 0$, and the lower limit is the horizontal axis which corresponds to $l_1 = \infty$. The minimum temperature of the angle section is more sensitive to changes in the value of ζ_1 than to changes in the value of ζ_2.

THERMAL STRESSES

In the following discussion, it is assumed that the section being considered is sufficiently far from the ends of the structural element that conditions at the ends do not affect the stress distribution. The stresses are determined by elementary elastic theory employing the assumptions that plane sections remain plane and that material properties do not change with temperature. The derivations of the stress equations are given in appendix B.

Thick Skin

The stress distribution in an unrestrained thick skin is given by the equation (see appendix B and ref. 4)

$$\sigma = -\frac{\alpha E}{1 - \mu}\left[(T - T_o) - \frac{1}{t}\int_{-\frac{t}{2}}^{\frac{t}{2}} (T - T_o)dy - 12\frac{y}{t^3}\int_{-\frac{t}{2}}^{\frac{t}{2}} (T - T_o)y\, dy\right] \quad (15a)$$

where

$$T = T(y)$$

with y being measured from the midplane of the plate. If y is measured from the unheated face of the plate, equation (15a) must be replaced by

$$\sigma = -\frac{\alpha E}{1 - \mu}\left[(T - T_o) + \frac{6}{t}\left(\frac{y}{t} - \frac{2}{3}\right)\int_0^t (T - T_o)dy + \frac{12}{t^2}\left(\frac{1}{2} - \frac{y}{t}\right)\int_0^t (T - T_o)y\, dy\right] \quad (15b)$$

Symmetrical heating.- If the skin is heated at the same rate on both surfaces, equation (15a) reduces to

$$\sigma = -\frac{\alpha E}{1 - \mu}\left[(T - T_o) - \frac{2}{t}\int_0^{\frac{t}{2}} (T - T_o)dy\right] \tag{16}$$

When equation (4a) is substituted into equation (16) and the indicated integration is performed, the result is

$$\sigma\left(\frac{1 - \mu}{\alpha E}\right)\frac{2k}{qt} = -\frac{\eta^2}{2} + \frac{1}{6} + \frac{2}{\pi^2}\sum_{n=1}^{\infty} (-1)^n \frac{\cos n\pi\eta}{n^2} e^{-n^2\pi^2\theta} \tag{17}$$

Stress distributions calculated by equation (17) are plotted in figures 15 and 16 in terms of dimensionless parameters; and, therefore, the results are applicable to any material for any thickness or time. In figures 15 and 16, $\eta = 0$ corresponds to the midplane of the plate. The stress distribution is symmetrical with respect to the midplane; therefore, the stresses are shown only for the half-depth of the plate.

Asymmetrical heating.- If the skin is heated on one surface only, the resulting unsymmetrical state requires that all terms of equation (15b) be included. When the temperature-distribution equation (4a) for this condition is substituted into equation (15b), the resulting stress equation is

$$\sigma\left(\frac{1 - \mu}{\alpha E}\right)\frac{2k}{qt} = \eta(1 - \eta) - \frac{1}{6} + \frac{4}{\pi^2}\sum_{n=1}^{\infty} (-1)^n \frac{\cos n\pi\eta}{n^2} e^{-n^2\pi^2\theta} +$$

$$\frac{48}{\pi^4}(1 - 2\eta) \sum_{n=1,3,5,\ldots}^{\infty} \frac{e^{-n^2\pi^2\theta}}{n^4} \tag{18}$$

Stress distributions calculated by equation (18) are plotted in figures 17 and 18 in terms of dimensionless parameters. It is interesting to note that, in certain regions of the skin, the thermal stresses reach maximum values at relatively short times during transient heating. In other regions the maximum stress is not reached until steady state exists. The inclusion of the last term in equation (15b), which term is obtained by satisfying moment equilibrium, causes the stresses to reach maximum values at relatively short times.

Angle, Channel, T-, and H-Sections

If it is assumed that material properties do not change with temperature and if elementary theory is employed, simple expressions may be derived for the stresses acting on unrestrained sections such as those shown in figure 11 with the heating as indicated. The stress equations are in terms of geometric properties, integrals involving the temperature distribution, and the local temperatures and are as follows: For the H-section,

$$\frac{\sigma_1}{\alpha E}\frac{k}{qt_2} = \frac{I_1}{\zeta_2\left(\frac{\zeta_1}{\zeta_2} + \frac{t_2}{t_1}\right)} - \phi_1 \tag{19a}$$

$$\frac{\sigma_2}{\alpha E}\frac{k}{qt_2} = \frac{I_1}{\zeta_2\left(\frac{\zeta_1}{\zeta_2} + \frac{t_2}{t_1}\right)} - \phi_2 \tag{19b}$$

for the T-section,

$$\frac{\sigma_1}{\alpha E}\frac{k}{qt_2} = \frac{6}{\zeta_2\left(\frac{\zeta_1}{\zeta_2} + \frac{4t_2}{t_1}\right)}\left\{\left(\frac{\zeta}{\zeta_1} - \frac{1}{3}\right)I_1 + \frac{\zeta_2}{\zeta_1^{\,2}}\left[\left(\frac{\zeta_1}{\zeta_2} + \frac{t_2}{t_1}\right)\left(2\frac{\zeta}{\zeta_1} - 1\right) - \frac{t_2}{t_1}\right]I_2\right\} - \phi_1 \tag{20a}$$

$$\frac{\sigma_2}{\alpha E}\frac{k}{qt_2} = \frac{6}{\zeta_2\left(\frac{\zeta_1}{\zeta_2} + \frac{4t_2}{t_1}\right)}\left(\frac{2}{3} I_1 + \frac{1}{\zeta_1} I_2\right) - \phi_2 \tag{20b}$$

for the channel section,

$$\frac{\sigma_1}{\alpha E}\frac{k}{qt_2} = \frac{6}{\zeta_2\left(4\frac{\zeta_1}{\zeta_2} + \frac{t_2}{t_1}\right)}\left(\frac{2}{3} I_1 + \frac{t_2}{t_1}\frac{I_3}{\zeta_2}\right) - \phi_1 \tag{21a}$$

$$\frac{\sigma_2}{\alpha E}\frac{k}{qt_2} = \frac{6}{\zeta_2\left(4\frac{\zeta_1}{\zeta_2} + \frac{t_2}{t_1}\right)}\left\{\left(\frac{\eta}{\zeta_2} - \frac{1}{3}\right)I_1 + \right.$$

$$\left.\left[2\frac{\zeta_1}{\zeta_2}\left(\frac{\eta}{\zeta_2} - 1\right) + \frac{1}{\zeta_2}\frac{t_2}{t_1}\left(2\frac{\eta}{\zeta_2} - 1\right)\right]I_3\right\} - \phi_2 \tag{21b}$$

for the angle section,

$$\frac{\sigma_1}{\alpha E}\frac{k}{qt_2} = \frac{3}{\zeta_1\zeta_2\left(\frac{\zeta_1}{\zeta_2} + \frac{t_2}{t_1}\right)}\left\{2\zeta_1\left(\frac{\zeta}{\zeta_1} - \frac{1}{3}\right)I_1 + \left[2\left(2\frac{\zeta}{\zeta_1} - 1\right) + \frac{t_2}{t_1}\frac{\zeta_2}{\zeta_1}\left(\frac{\zeta}{\zeta_1} - 1\right)\right]I_2 + \right.$$

$$\left.\frac{t_2}{t_1}\frac{\zeta_1}{\zeta_2}\left(3\frac{\zeta}{\zeta_1} - 1\right)I_3\right\} - \phi_1 \tag{22a}$$

$$\frac{\sigma_2}{\alpha E}\frac{k}{qt_2} = \frac{3}{\zeta_1\zeta_2\left(\frac{\zeta_1}{\zeta_2} + \frac{t_2}{t_1}\right)}\left\{2\zeta_1\left(\frac{\eta}{\zeta_2} - \frac{1}{3}\right)I_1 + \left(3\frac{\eta}{\zeta_2} - 1\right)I_2 + \right.$$

$$\left.\frac{t_2}{t_1}\frac{\zeta_1}{\zeta_2}\left[2\left(2\frac{\eta}{\zeta_2} - 1\right) + \frac{t_1}{t_2}\frac{\zeta_1}{\zeta_2}\left(\frac{\eta}{\zeta_2} - 1\right)\right]I_3\right\} - \phi_2 \qquad (22b)$$

The integrals I_1, I_2, and I_3 are defined as follows:

$$I_1 = \frac{k}{qt_2} I_1' \qquad (23)$$

where

$$\left.\begin{aligned} I_1' &= \int_0^{\zeta_1} (T_1 - T_o)d\zeta + \frac{t_2}{t_1}\int_0^{\zeta_2} (T_2 - T_o)d\eta \\ I_2' &= \int_0^{\zeta_1} (T_1 - T_o)(\zeta - \zeta_1)d\zeta \\ I_3' &= \int_0^{\zeta_2} (T_2 - T_o)(\eta - \zeta_2)d\eta \end{aligned}\right\} \qquad (24)$$

The quantities I_2 and I_3 have been calculated for all possible combinations of $\frac{t_2}{t_1} = 1$, 2, and 4, $\zeta_1 = 5$, 10, and 20, and $\zeta_2 = 10$, 20, and 30, and are plotted in figures 19 and 20. Because of its simplicity, I_1 is given only in the form of an equation. (See appendix B.)

EXAMPLE

Temperature Distribution in an Angle

In order to illustrate the results of the analysis described herein, an example is presented. The case chosen is $\frac{t_2}{t_1} = 1$, $\zeta_1 = \zeta_2 = 10$. For the example chosen $\frac{\zeta_1}{\zeta_2} = 1$ and the characteristic values are (from eq. (8))

$$\beta_n = \frac{n\pi}{2\zeta_1} \qquad (n = 1, 3, 5, \ldots)$$

The temperature distribution was calculated by using equations (7) and is given in figures 21 and 22 as a function of time and space, respectively. This particular case reaches quasi-steady-state conditions rather rapidly ($\theta \approx 150$). Note also that the temperature at the junction of the two elements that make up the basic angle section is a linear function of time and is the average temperature of the section.

Stress Distribution

The quasi-steady-state stresses were calculated for the four cases shown in figure 11 by assuming $\theta = \infty$ and using equations (19) to (22). The results are presented in dimensionless form in figure 23. The results, which are for unrestrained expansion, indicate that, for the case chosen, if the H-section is divided along either line of symmetry, the absolute value of the maximum stress on the resulting section is one-half that of the H-section. If the H-section is quartered, the absolute value of the maximum stress on the resulting section is one-fourth that of the H-section.

CONCLUDING REMARKS

Solutions for the temperature distributions and thermal stresses of structural elements such as plates, channel, angle, T-, and H-sections when subjected to constant heating rates have been presented. These solutions and charts obtained from them have been found to be useful in analyzing and correlating experimental data. In addition to temperature distributions, thermal stresses are given in forms involving simple integral functions of the temperatures.

The temperatures of selected points on the element cross sections have been calculated and presented in dimensionless form for several geometric configurations. The temperature integrals involved in the thermal stress equations have been calculated for the same configurations and are also presented in dimensionless forms. By the use of dimensionless temperature and stress parameters it is possible to employ the results for different materials and heating rates.

A detailed distribution of temperature and stress is given for a selected case in order to provide some insight into the nature of the variation of temperature and stress on the cross section.

Langley Aeronautical Laboratory,
National Advisory Committee for Aeronautics,
Langley Field, Va., May 27, 1958.

APPENDIX A

TEMPERATURE DISTRIBUTION

Thick Skin

In figure 3, a schematic diagram of a thick skin heated on one face is shown. It is assumed that there is a variation of temperature through the thickness but no variation in the plane of the skin. The governing differential equation is

$$\frac{\partial T}{\partial \tau} = \frac{k}{cw} \frac{\partial^2 T}{\partial y^2} \tag{A1}$$

In addition, it is assumed that there is a constant heat flux on one face $(y = t)$ and that there is no heat loss from the other face $(y = 0)$. The resulting boundary conditions are

$$\left.\frac{\partial T}{\partial y}\right|_{t,\tau} = \frac{q}{k} \tag{A2a}$$

$$\left.\frac{\partial T}{\partial y}\right|_{0,\tau} = 0 \tag{A2b}$$

The initial condition is

$$T(y,0) = T_0 \tag{A3}$$

Expressed in a dimensionless form, equation (A1) becomes

$$\frac{\partial T}{\partial \theta} = \frac{\partial^2 T}{\partial \eta^2} \tag{A4}$$

and equations (A2) are written as

$$\left.\frac{\partial T}{\partial \eta}\right|_{1,\theta} = \frac{qt}{k} \tag{A5a}$$

$$\left.\frac{\partial T}{\partial \eta}\right|_{0,\theta} = 0 \tag{A5b}$$

where

$$\left.\begin{aligned} \theta &= \frac{k\tau}{cwt^2} \\ \eta &= \frac{y}{t} \end{aligned}\right\} \tag{A6}$$

By employing the Laplace transformation the differential equation (A4) and the boundary-condition equations (A5) may be written as

$$\frac{d^2\overline{T}}{d\eta^2} - s\overline{T} + T_o = 0 \tag{A7}$$

and

$$\left.\frac{d\overline{T}}{d\eta}\right|_{1} = \frac{qt}{ks} \tag{A8a}$$

$$\left.\frac{d\overline{T}}{d\eta}\right|_{0} = 0 \tag{A8b}$$

where

$$\overline{T}(\eta,s) = L\left\{T(\eta,\theta)\right\} \tag{A9}$$

The solution of equation (A7) subject to the boundary conditions (A8) is

$$\overline{T} = \frac{T_o}{s} + \frac{qt}{k}\,\frac{\cosh\sqrt{s}\eta}{s^{3/2}\sinh\sqrt{s}} \tag{A10}$$

An inverse transform of equation (A10) and the required temperature expression is

$$T = T_o + \frac{qt}{k}\left[\theta + \frac{\eta^2}{2} - \frac{1}{6} - \frac{2}{\pi^2}\sum_{n=1}^{\infty}(-1)^n\,\frac{\cos n\pi\eta}{n^2}\,e^{-n^2\pi^2\theta}\right] \tag{A11}$$

An alternate form of solution which converges rapidly for small values of θ is obtained by writing equation (A10) in the following equivalent form

$$\overline{T} = \frac{T_o}{s} + \frac{qt}{k}\,\frac{1}{s^{3/2}}\sum_{n=1,3,5,\ldots}^{\infty}\left[e^{-\sqrt{s}(n-\eta)} + e^{-\sqrt{s}(n+\eta)}\right] \tag{A12}$$

The inverse transform of equation (A12) is

$$T = T_o + \frac{qt}{k}\sum_{n=1,3,5,\ldots}^{\infty}\left[2\sqrt{\frac{\theta}{\pi}}\left\{\exp\left[-\frac{(n-\eta)^2}{4\theta}\right] + \exp\left[-\frac{(n+\eta)^2}{4\theta}\right]\right\} - \left\{(n-\eta)\operatorname{erfc}\left(\frac{n-\eta}{2\sqrt{\theta}}\right) + (n+\eta)\operatorname{erfc}\left(\frac{n+\eta}{2\sqrt{\theta}}\right)\right\}\right] \tag{A13}$$

The average temperature parameter of the thick skin is found by rearranging equation (A11) and integrating over the thickness, or

$$\phi_{av} = \int_0^1 \phi \, d\eta \tag{A14}$$

yielding

$$\phi_{av} = \theta \tag{A15}$$

The nondimensional temperature difference, defined as

$$\Delta\phi = \phi\Big|_{1,\theta} - \phi\Big|_{0,\theta} \tag{A16}$$

may be found by using equation (A11) and is

$$\Delta\phi = \frac{1}{2} - \frac{4}{\pi^2} \sum_{n=1,3,5,\ldots}^{\infty} \frac{e^{-n^2\pi^2\theta}}{n^2} \tag{A17}$$

It is obvious that, as θ becomes large, the nondimensional temperature difference increases until it reaches its maximum value of

$$\Delta\phi = \frac{1}{2} \tag{A18}$$

or

$$\Delta T = \frac{1}{2} \frac{qt}{k} \tag{A19}$$

at an infinite time.

Angle, Channel, T-, and H-Sections

The idealized angle section of figure 10(b) is next considered. It is assumed that there is no variation of temperature through the thicknesses t_1 and t_2 and that there is no heat loss through the unheated faces. Because of the discontinuity in heating and thickness, the section is considered as two elements wherein the temperatures are governed by the following equations:

$$\frac{\partial T_1}{\partial \tau} = \left(\frac{k}{cw}\right)_1 \frac{\partial^2 T_1}{\partial y^2} \tag{A20a}$$

$$\frac{\partial T_2}{\partial \tau} = \left(\frac{k}{cw}\right)_2 \frac{\partial^2 T_2}{\partial x^2} + \frac{q}{(cwt)_2} \tag{A20b}$$

subject to the following boundary conditions

$$\frac{\partial T_1}{\partial y}(0,\tau) = 0 \tag{A21a}$$

$$(kt)_1 \frac{\partial T_1}{\partial y}(l_1,\tau) = -(kt)_2 \frac{\partial T_2}{\partial x}(l_2,\tau) \tag{A21b}$$

$$T_1(l_1,\tau) = T_2(l_2,\tau) \tag{A21c}$$

$$\frac{\partial T_2}{\partial x}(0,\tau) = 0 \tag{A21d}$$

The initial condition is

$$T_1(y,0) = T_2(x,0) = T_o \tag{A22}$$

If it is assumed that the two elements are of the same material, the following dimensionless equations may be written to replace equations (A20) and (A21):

$$\frac{\partial T_1}{\partial \theta} = \frac{\partial^2 T_1}{\partial \zeta^2} \tag{A23a}$$

$$\frac{\partial T_2}{\partial \theta} = \frac{\partial^2 T_2}{\partial \eta^2} + \frac{qt_2}{k} \tag{A23b}$$

and

$$\frac{\partial T_1}{\partial \zeta}(0,\theta) = 0 \tag{A24a}$$

$$\frac{t_1}{t_2} \frac{\partial T_1}{\partial \zeta}(\zeta_1,\theta) = - \frac{\partial T_2}{\partial \eta}(\zeta_2,\theta) \tag{A24b}$$

$$T_1(\zeta_1,\theta) = T_2(\zeta_2,\theta) \tag{A24c}$$

$$\frac{\partial T_2}{\partial \eta}(0,\theta) = 0 \tag{A24d}$$

where

$$\left.\begin{aligned} \theta &= \frac{k\tau}{cwt_2^2} \\ \zeta &= \frac{y}{t_2} \qquad \zeta_1 = \frac{l_1}{t_2} \\ \eta &= \frac{x}{t_2} \qquad \zeta_2 = \frac{l_2}{t_2} \end{aligned}\right\} \tag{A25}$$

If the Laplace transformation is employed, the differential equations (A23) and the boundary-condition equations (A24) become

$$\frac{d^2\overline{T}_1}{d\zeta^2} - s\overline{T}_1 + T_o = 0 \tag{A26a}$$

$$\frac{d^2\overline{T}_2}{d\eta^2} - s\overline{T}_2 + T_o + \frac{1}{s}\frac{qt_2}{k} = 0 \tag{A26b}$$

and

$$\frac{d\overline{T}_1}{d\zeta}(0) = 0 \tag{A27a}$$

$$\frac{t_1}{t_2}\frac{d\overline{T}_1}{d\zeta}(\zeta_1) = -\frac{d\overline{T}_2}{d\eta}(\zeta_2) \tag{A27b}$$

$$\overline{T}_1(\zeta_1) = \overline{T}_2(\zeta_2) \tag{A27c}$$

$$\frac{d\overline{T}_2}{d\eta}(0) = 0 \tag{A27d}$$

The solutions of the transformed differential equations (A26) subject to the boundary conditions (A27) are

$$\overline{T}_1 = \frac{T_o}{s} + \frac{qt_2}{s^2k}\frac{\frac{t_2}{t_1}\sinh\sqrt{s}\zeta_2\cosh\sqrt{s}\zeta}{\left(\sinh\sqrt{s}\zeta_1\cosh\sqrt{s}\zeta_2 + \frac{t_2}{t_1}\sinh\sqrt{s}\zeta_2\cosh\sqrt{s}\zeta_1\right)} \tag{A28a}$$

$$\bar{T}_2 = \frac{T_o}{s} + \frac{qt_2}{s^2 k}\left(1 - \frac{\sinh\sqrt{s}\zeta_1 \cosh\sqrt{s}\eta}{\sinh\sqrt{s}\zeta_1 \cosh\sqrt{s}\zeta_2 + \frac{t_2}{t_1}\sinh\sqrt{s}\zeta_2 \cosh\sqrt{s}\zeta_1}\right) \qquad \text{(A28b)}$$

The poles of equations (A28) are a pole of order 2 at $s = 0$ and simple poles at $s = -\beta_n^2$, where the terms β_n are roots of the following transcendental equation:

$$\sin \beta_n\zeta_1 \cos \beta_n\zeta_2 + \frac{t_2}{t_1} \sin \beta_n\zeta_2 \cos \beta_n\zeta_1 = 0 \qquad \text{(A29)}$$

For $\cos \beta_n\zeta_1 \cos \beta_n\zeta_2 \neq 0$, β_n is given by the following equation:

$$\tan \beta_n\zeta_1 + \frac{t_2}{t_1} \tan \beta_n\zeta_2 = 0 \qquad \text{(A30)}$$

In the present paper the values $\frac{\zeta_2}{\zeta_1} = 1$ and 3 occur. For the case $\frac{\zeta_2}{\zeta_1} = 1$, β_n is given by

$$\cos \beta_n\zeta_1 = 0 \qquad (n = 1, 3, 5, \ldots)$$

or

$$\beta_n = \frac{n\pi}{2\zeta_1} \qquad (n = 1, 3, 5, \ldots) \qquad \text{(A31)}$$

For $\dfrac{\zeta_2}{\zeta_1} = 3$, there are three sets of β_n. Two of the sets are roots of equations (A30) and (A31), and the third set is given by

$$\cos \beta_n \zeta_2 = 0 \qquad (n = 1, 5, 7, 11, \ldots)$$

or

$$\beta_n = \frac{n\pi}{6\zeta_1} \qquad (n = 1, 5, 7, 11, \ldots) \tag{A32}$$

By a formal application of the inversion integral the required temperature distributions are found to be

$$(T_1 - T_o)\frac{k}{qt_2} = \frac{t_2}{t_1}\left[\frac{\theta}{\dfrac{\zeta_1}{\zeta_2} + \dfrac{t_2}{t_1}} + \frac{\dfrac{1}{2}\zeta^2}{\dfrac{\zeta_1}{\zeta_2} + \dfrac{t_2}{t_1}} - \frac{\dfrac{1}{6}\dfrac{\zeta_1}{\zeta_2}\left(\zeta_1^{\,2} + 2\zeta_2^{\,2}\right) + \dfrac{1}{2}\zeta_1^{\,2}\dfrac{t_2}{t_1}}{\left(\dfrac{\zeta_1}{\zeta_2} + \dfrac{t_2}{t_1}\right)^2} - \right.$$

$$\left. \frac{2}{\zeta_2}\sum_{n=1}^{\infty} \frac{\dfrac{e^{-\beta_n^{\,2}\theta}}{\beta_n^{\,3}}}{\left(\dfrac{\zeta_1}{\zeta_2} + \dfrac{t_2}{t_1}\right)\cot \beta_n\zeta_2 - \left(1 + \dfrac{\zeta_1}{\zeta_2}\dfrac{t_2}{t_1}\right)\tan \beta_n\zeta_1} \frac{\cos \beta_n\zeta}{\cos \beta_n\zeta_1}\right] \tag{A33a}$$

$$(T_2 - T_o)\frac{k}{qt_2} = \frac{t_2}{t_1}\left[\frac{\theta}{\frac{\zeta_1}{\zeta_2} + \frac{t_2}{t_1}} - \frac{\frac{1}{2}\frac{\zeta_1}{\zeta_2}\frac{t_1}{t_2}\eta^2}{\frac{\zeta_1}{\zeta_2} + \frac{t_2}{t_1}} + \frac{\frac{1}{6}\frac{\zeta_1}{\zeta_2}\left({\zeta_2}^2 + 2{\zeta_1}^2\right) + \frac{1}{2}{\zeta_1}^2\frac{t_1}{t_2}}{\left(\frac{\zeta_1}{\zeta_2} + \frac{t_2}{t_1}\right)^2} + \right.$$

$$\left.\frac{t_1}{t_2}\frac{2}{\zeta_2}\sum_{n=1}^{\infty}\frac{\frac{e^{-{\beta_n}^2\theta}}{{\beta_n}^3}}{\left(\frac{\zeta_1}{\zeta_2} + \frac{t_2}{t_1}\right)\cot\beta_n\zeta_1 - \left(1 + \frac{\zeta_1}{\zeta_2}\frac{t_2}{t_1}\right)\tan\beta_n\zeta_2}\frac{\cos\beta_n\eta}{\cos\beta_n\zeta_2}\right] \tag{A33b}$$

Because equations (A33) converge slowly for short times, it is advisable to derive a short-time solution for the present problem. This derivation can be made most readily by appropriate substitutions in equations (A28). For small times (large values of s) assume that

$$\left.\begin{aligned}\sinh\sqrt{s}\zeta_1 &= \cosh\sqrt{s}\zeta_1 = \frac{1}{2}e^{\sqrt{s}\zeta_1}\\ \sinh\sqrt{s}\zeta_2 &= \cosh\sqrt{s}\zeta_2 = \frac{1}{2}e^{\sqrt{s}\zeta_2}\end{aligned}\right\} \tag{A34}$$

and

$$\left.\begin{aligned}\cosh\sqrt{s}\zeta &= \frac{1}{2}\left(e^{\sqrt{s}\zeta} + e^{-\sqrt{s}\zeta}\right)\\ \cosh\sqrt{s}\eta &= \frac{1}{2}\left(e^{\sqrt{s}\eta} + e^{-\sqrt{s}\eta}\right)\end{aligned}\right\} \tag{A35}$$

If the quantities defined in equations (A35) are substituted into equations (A28), the result is

$$\bar{T}_1 = \frac{T_o}{s} + \frac{qt_2}{k} \frac{1}{1 + \frac{t_1}{t_2}} \frac{1}{s^2}\left[e^{-\sqrt{s}(\zeta_1-\zeta)} + e^{-\sqrt{s}(\zeta_1+\zeta)}\right] \tag{A36a}$$

$$\bar{T}_2 = \frac{T_o}{s} + \frac{qt_2}{k} \frac{1}{s^2}\left\{1 - \frac{1}{1 + \frac{t_2}{t_1}}\left[e^{-\sqrt{s}(\zeta_2-\eta)} + e^{-\sqrt{s}(\zeta_2+\eta)}\right]\right\} \tag{A36b}$$

The inverse transforms of equations (A36) can be written as (ref. 5)

$$\begin{aligned}(T_1 - T_o)\frac{k}{qt_2} = \frac{1}{1 + \frac{t_1}{t_2}} \Bigg\{&\left[\theta + \frac{(\zeta_1 - \zeta)^2}{2}\right]\operatorname{erfc}\left(\frac{\zeta_1 - \zeta}{2\sqrt{\theta}}\right) - \\ &(\zeta_1 - \zeta)\sqrt{\frac{\theta}{\pi}} \exp\left[-\frac{(\zeta_1 - \zeta)^2}{4\theta}\right] + \\ &\left[\theta + \frac{(\zeta_1 + \zeta)^2}{2}\right]\operatorname{erfc}\left(\frac{\zeta_1 + \zeta}{2\sqrt{\theta}}\right) - \\ &(\zeta_1 + \zeta)\sqrt{\frac{\theta}{\pi}} \exp\left[-\frac{(\zeta_1 + \zeta)^2}{4\theta}\right]\Bigg\}\end{aligned} \tag{A37a}$$

$$\left(T_2 - T_o\right)\frac{k}{qt_2} = \theta - \frac{1}{1 + \frac{t_2}{t_1}}\left\{\left[\theta + \frac{\left(\zeta_2 - \eta\right)^2}{2}\right]\mathrm{erfc}\left(\frac{\zeta_2 - \eta}{2\sqrt{\theta}}\right) - \right.$$

$$\left(\zeta_2 - \eta\right)\sqrt{\frac{\theta}{\pi}}\exp\left[-\frac{\left(\zeta_2 - \eta\right)^2}{4\theta}\right] +$$

$$\left[\theta + \frac{\left(\zeta_2 + \eta\right)^2}{2}\right]\mathrm{erfc}\left(\frac{\zeta_2 + \eta}{2\sqrt{\theta}}\right) -$$

$$\left.\left(\zeta_2 + \eta\right)\sqrt{\frac{\theta}{\pi}}\exp\left[-\frac{\left(\zeta_2 + \eta\right)^2}{4\theta}\right]\right\} \tag{A37b}$$

APPENDIX B

THERMAL STRESSES

In the following discussion, secondary effects are neglected; that is, it is assumed that the section under consideration is sufficiently removed from the ends of the structural element that the stress distribution is not influenced by the stress-free condition at the ends. All the stresses are determined by elementary elastic theory employing the assumptions that plane sections remain plane and that material properties do not change with temperature.

If plane sections remain plane, the axial strain at any point can be written as

$$\epsilon = a + bx + cy \tag{B1}$$

The stress-strain relation is

$$\epsilon = \frac{\sigma}{E^*} + \alpha(T - T_o) \tag{B2}$$

where, for a free plate with temperature variation through the thickness only,

$$E^* = \frac{E}{1 - \mu} \tag{B3}$$

and for plane stress

$$E^* = E \tag{B4}$$

The stress can be expressed as

$$\sigma = E^*\left[a + bx + cy - \alpha(T - T_o)\right] \tag{B5}$$

The equilibrium equations which must be satisfied are

$$\left.\begin{aligned} \int_A \sigma\, dA &= 0 \\ \int_A \sigma x\, dA &= 0 \\ \int_A \sigma y\, dA &= 0 \end{aligned}\right\} \tag{B6}$$

If equation (B5) is substituted into equations (B6) and the indicated integrations are performed, there is obtained the following general set of equations for determining the values of the constants a, b, and c:

$$\left.\begin{aligned} A_1a + B_1b + C_1c &= \alpha I_1' \\ A_2a + B_2b + C_2c &= \alpha I_2' \\ A_3a + B_3b + C_3c &= \alpha I_3' \end{aligned}\right\} \tag{B7}$$

The constants A, B, and C are known functions of the geometry of the particular section under consideration; I_1', I_2', and I_3' are integrals involving the temperature.

Thick Skin

The thick skin considered in the present paper experiences variation of temperature in the thickness direction only. The coefficients for equation (B7) for the free plate are

$$\left.\begin{matrix} A_1 = 1 & B_1 = 0 & C_1 = \dfrac{t}{2} \\ A_2 = 0 & B_2 = 0 & C_2 = 0 \\ A_3 = \dfrac{t}{2} & B_3 = 0 & C_3 = \dfrac{t^2}{3} \end{matrix}\right\} \tag{B8}$$

The right-hand sides of the equations (B7) are

$$\left.\begin{aligned}
\alpha I_1' &= \frac{\alpha}{t}\int_0^t (T - T_0)dy \\
\alpha I_2' &= 0 \\
\alpha I_3' &= \frac{\alpha}{t}\int_0^t (T - T_0)y\,dy
\end{aligned}\right\} \tag{B9}$$

When equations (B7) are solved for the coefficients a and c which are then substituted into equation (B5), the stress is

$$\sigma = -\frac{\alpha E}{1 - \mu}\left[(T - T_0) + \frac{6}{t}\left(\frac{y}{t} - \frac{2}{3}\right)\int_0^t (T - T_0)dy + \frac{12}{t^2}\left(\frac{1}{2} - \frac{y}{t}\right)\int_0^t (T - T_0)y\,dy\right] \tag{B10}$$

where y is measured from the unheated surface. If the origin is transferred to the midplane of the plate; equation (15a) is obtained.

If equation (A11) is substituted in equation (B10), the resulting stress equation for the unsymmetrically heated plate is

$$\sigma\left(\frac{1 - \mu}{\alpha E}\right)\frac{2k}{qt} = \eta(1 - \eta) - \frac{1}{6} + \frac{4}{\pi^2}\sum_{n=1}^{\infty}(-1)^n \frac{\cos n\pi\eta}{n^2} e^{-n^2\pi^2\theta} + \frac{48}{\pi^4}(1 - 2\eta)\sum_{n=1,3,5,\ldots}^{\infty}\frac{e^{-n^2\pi^2\theta}}{n^4} \tag{B11}$$

If the skin is heated symmetrically with respect to its midplane and there is no variation of temperature in the plane of the skin, the last two of equations (B6) are automatically satisfied and b = c = 0.

The first of equations (B6) must be employed to determine a. When this is done, the stress is

$$\sigma = -\frac{\alpha E}{1 - \mu}\left[(T - T_0) - \frac{2}{t}\int_0^{\frac{t}{2}} (T - T_0)dy\right] \tag{B12}$$

where y is measured from the midplane of the plate.

If equation (A11) is substituted into equation (B12), the resulting stress equation for the symmetrically heated skin is

$$\sigma\left(\frac{1 - \mu}{\alpha E}\right)\frac{2k}{qt} = -\frac{\eta^2}{2} + \frac{1}{6} + \frac{2}{\pi^2}\sum_{n=1}^{\infty} (-1)^n \frac{\cos n\pi\eta}{n^2} e^{-n^2\pi^2\theta} \tag{B13}$$

Angle, Channel, T-, and H-Sections

The thicknesses of the sections of figure 11 are small enough to permit the assumption of plane stress. For the general case, the coefficients A, B, and C of equation (B7) are as follows:

$$\left.\begin{aligned}
A_1 &= \zeta_2\left(\frac{\zeta_1}{\zeta_2} + \frac{t_2}{t_1}\right) & B_1 &= t_2\zeta_1\zeta_2\left(\frac{\zeta_1}{2\zeta_2} + \frac{t_2}{t_1}\right) & C_1 &= \frac{t_2\zeta_2^2}{2}\left(2\frac{\zeta_1}{\zeta_2} + \frac{t_2}{t_1}\right) \\
A_2 &= -\frac{\zeta_1^2}{2} & B_2 &= -\frac{t_2\zeta_1^3}{6} & C_2 &= -\frac{t_2\zeta_1^2\zeta_2}{2} \\
A_3 &= -\frac{\zeta_2^2}{2} & B_3 &= -\frac{t_2\zeta_1\zeta_2^2}{2} & C_3 &= -\frac{t_2\zeta_2^3}{6}
\end{aligned}\right\} \tag{B14}$$

The right-hand sides of equations (B7) are

$$\left.\begin{aligned}
\alpha I_1' &= \alpha\left[\int_0^{\zeta_1} (T_1 - T_o)d\zeta + \frac{t_2}{t_1}\int_0^{\zeta_2} (T_2 - T_o)d\eta\right] \\
\alpha I_2' &= \alpha \int_0^{\zeta_1} (T_1 - T_o)(\zeta - \zeta_1)d\zeta \\
\alpha I_3' &= \alpha \int_0^{\zeta_2} (T_2 - T_o)(\eta - \zeta_2)d\eta
\end{aligned}\right\} \qquad \text{(B15)}$$

The H-section of figure 11 is the simplest case because of double symmetry. In this case the constants b and c are zero; therefore,

$$\frac{\sigma_1}{\alpha E} = \frac{I_1'}{\zeta_2\left(\dfrac{\zeta_1}{\zeta_2} + \dfrac{t_2}{t_1}\right)} - (T_1 - T_o) \qquad \text{(B16a)}$$

$$\frac{\sigma_2}{\alpha E} = \frac{I_1'}{\zeta_2\left(\dfrac{\zeta_1}{\zeta_2} + \dfrac{t_2}{t_1}\right)} - (T_2 - T_o) \qquad \text{(B16b)}$$

For the T-section of figure 11, the constant b equals zero and the stresses are

$$\frac{\sigma_1}{\alpha E} = \frac{6}{\zeta_2\left(\dfrac{\zeta_1}{\zeta_2} + 4\,\dfrac{t_2}{t_1}\right)}\left\{\left(\frac{\zeta}{\zeta_1} - \frac{1}{3}\right)I_1' + \frac{\zeta_2}{{\zeta_1}^2}\left[\left(\frac{\zeta_1}{\zeta_2} + \frac{t_2}{t_1}\right)\left(2\,\frac{\zeta}{\zeta_1} - 1\right) - \frac{t_2}{t_1}\right]I_2'\right\} - (T_1 - T_o) \qquad \text{(B17a)}$$

$$\frac{\sigma_2}{\alpha E} = \frac{6}{\zeta_2\left(\frac{\zeta_1}{\zeta_2} + 4\frac{t_2}{t_1}\right)}\left(\frac{2}{3} I_1' + \frac{1}{\zeta_1} I_2'\right) - (T_2 - T_o) \tag{B17b}$$

For the channel section of figure 11, the constant c equals zero and the stresses are

$$\frac{\sigma_1}{\alpha E} = \frac{6}{\zeta_2\left(4\frac{\zeta_1}{\zeta_2} + \frac{t_2}{t_1}\right)}\left(\frac{2}{3} I_1' + \frac{t_2}{t_1}\frac{I_3'}{\zeta_2}\right) - (T_1 - T_o) \tag{B18a}$$

$$\frac{\sigma_2}{\alpha E} = \frac{6}{\zeta_2\left(4\frac{\zeta_1}{\zeta_2} + \frac{t_2}{t_1}\right)}\left\{\left(\frac{\eta}{\zeta_2} - \frac{1}{3}\right)I_1' + \left[2\frac{\zeta_1}{\zeta_2^{2}}\left(\frac{\eta}{\zeta_2} - 1\right) + \frac{1}{\zeta_2}\frac{t_2}{t_1}\left(\frac{2\eta}{\zeta_2} - 1\right)\right] I_3'\right\} - (T_2 - T_o) \tag{B18b}$$

The angle section of figure 11 requires the use of all the constants, and the stresses are

$$\frac{\sigma_1}{\alpha E} = \frac{3}{\zeta_1\zeta_2\left(\frac{\zeta_1}{\zeta_2} + \frac{t_2}{t_1}\right)}\left\{2\zeta_1\left(\frac{\zeta}{\zeta_1} - \frac{1}{3}\right)I_1' + \left[2\left(2\frac{\zeta}{\zeta_1} - 1\right) + \frac{t_2}{t_1}\frac{\zeta_2}{\zeta_1}\left(\frac{\zeta}{\zeta_1} - 1\right)\right] I_2' + \frac{t_2}{t_1}\frac{\zeta_1}{\zeta_2}\left(3\frac{\zeta}{\zeta_1} - 1\right)I_3'\right\} - (T_1 - T_o) \tag{B19a}$$

$$\frac{\sigma_2}{\alpha E} = \frac{3}{\zeta_1\zeta_2\left(\frac{\zeta_1}{\zeta_2} + \frac{t_2}{t_1}\right)}\left\{2\zeta_1\left(\frac{\eta}{\zeta_2} - \frac{1}{3}\right)I_1' + \left(3\frac{\eta}{\zeta_2} - 1\right)I_2' + \right.$$

$$\left.\frac{t_2}{t_1}\frac{\zeta_1}{\zeta_2}\left[2\left(2\frac{\eta}{\zeta_2} - 1\right) + \frac{t_1}{t_2}\frac{\zeta_1}{\zeta_2}\left(\frac{\eta}{2} - 1\right)\right]I_3'\right\} - (T_2 - T_o) \qquad \text{(B19b)}$$

In order to keep the results in a dimensionless form, rather than employing the integrals defined by equations (15), integrals defined as follows are used:

$$I_i = I_i' \frac{k}{qt_2} \qquad \text{(B20)}$$

After the indicated integrations are performed, the equations for I_1, I_2, and I_3 are as follows:

$$I_1 = \frac{t_2}{t_1}\zeta_2\theta \qquad \text{(B21a)}$$

$$I_2 = -\frac{\frac{t_2}{t_1}\frac{\zeta_1^2}{2}}{\frac{\zeta_1}{\zeta_2} + \frac{t_2}{t_1}}\left[\theta + \frac{\zeta_1^2}{12} - \frac{\frac{1}{6}\frac{\zeta_1}{\zeta_2}\left(\zeta_1^2 + 2\zeta_2^2\right) + \frac{1}{2}\zeta_1^2\frac{t_2}{t_1}}{\frac{\zeta_1}{\zeta_2} + \frac{t_2}{t_1}}\right] -$$

$$\frac{t_2}{t_1}\frac{2}{\zeta_2}\sum_{n=1}^{\infty}\frac{\frac{e^{-\beta_n^2\theta}}{\beta_n^5}}{\left(\frac{\zeta_1}{\zeta_2} + \frac{t_2}{t_1}\right)\cot\beta_n\zeta_2 - \left(1 + \frac{\zeta_1}{\zeta_2}\frac{t_2}{t_1}\right)\tan\beta_n\zeta_1}\left(1 - \frac{1}{\cos\beta_n\zeta_1}\right)$$

$$\text{(B21b)}$$

$$I_3 = -\frac{\frac{t_2}{t_1}\frac{\zeta_1^2}{2}}{\frac{\zeta_1}{\zeta_2}+\frac{t_2}{t_1}}\left[\theta - \frac{1}{12}\frac{t_1}{t_2}\zeta_1\zeta_2 + \frac{\frac{1}{6}\frac{\zeta_1}{\zeta_2}\left(\zeta_2^2 + 2\zeta_1^2\right) + \frac{1}{2}\zeta_1^2\frac{t_1}{t_2}}{\frac{\zeta_1}{\zeta_2}+\frac{t_2}{t_1}}\right] +$$

$$\frac{2}{\zeta_2}\sum_{n=1}^{\infty}\frac{\frac{e^{-\beta_n^2\theta}}{\beta_n^5}}{\left(\frac{\zeta_1}{\zeta_2}+\frac{t_2}{t_1}\right)\cot\beta_n\zeta_1 - \left(1+\frac{\zeta_1}{\zeta_2}\frac{t_2}{t_1}\right)\tan\beta_n\zeta_2}\left(1 - \frac{1}{\cos\beta_n\zeta_2}\right) \tag{B21c}$$

The stresses may now be written in a dimensionless form by multiplying the left-hand sides of equations (B16), (B17), (B18), and (B19) by k/qt_2 and replacing I_1' in the right-hand sides by I_1. The values of I_2 and I_3 were calculated for all combinations of $\frac{t_2}{t_1} = 1$, 2, and 4, $\zeta_1 = 5$, 10, and 20, and $\zeta_2 = 10$, 20, and 30, by using either equation (A30), equation (A31), or equations (A30), (A31), and (A32), which define the characteristic value β_n. For a given case I_1 can be computed from equation (B21a).

REFERENCES

1. Brooks, William A., Jr., Griffith, George E., and Strass, H. Kurt: Two Factors Influencing Temperature Distributions and Thermal Stresses in Structures. NACA TN 4052, 1957.

2. Carslaw, H. S., and Jaeger, J. C.: Conduction of Heat in Solids. The Clarendon Press (Oxford), 1947, p. 104.

3. Pohle, Frederick V., and Berman, Irwin: Thermal Stresses in Airplane Wings Under Constant Heat Input. Ch. 2 of Induction Heating and Theory in the Solution of Transient Problems of Aircraft Structures. WADC Tech. Rep. 56-145 (ASTIA Doc. No. AD 97210), U. S. Air Force, Aug. 1956, pp. 35-79.

4. Timoshenko, S.: Theory of Elasticity. First ed., McGraw-Hill Book Co., Inc., 1934, p. 210.

5. Churchill, Ruel V.: Modern Operational Mathematics in Engineering. McGraw-Hill Book Co., Inc., 1944.

TABLE I.- TYPICAL MATERIAL PROPERTIES

Material	T, °F (a)	w, lb/cu ft	c, Btu/lb-°F	k, Btu/sec-ft-°F
Aluminum alloy	250	173	0.220	0.0228
Magnesium alloy	250	110	.247	.0145
Copper	400	570	.097	.0583
Titanium alloy	500	280	.145	.0021
Stainless steel	600	490	.130	.0031
Monel	700	520	.118	.0044
Inconel X	800	505	.128	.0028

[a]Representative of average temperatures in typical applications.

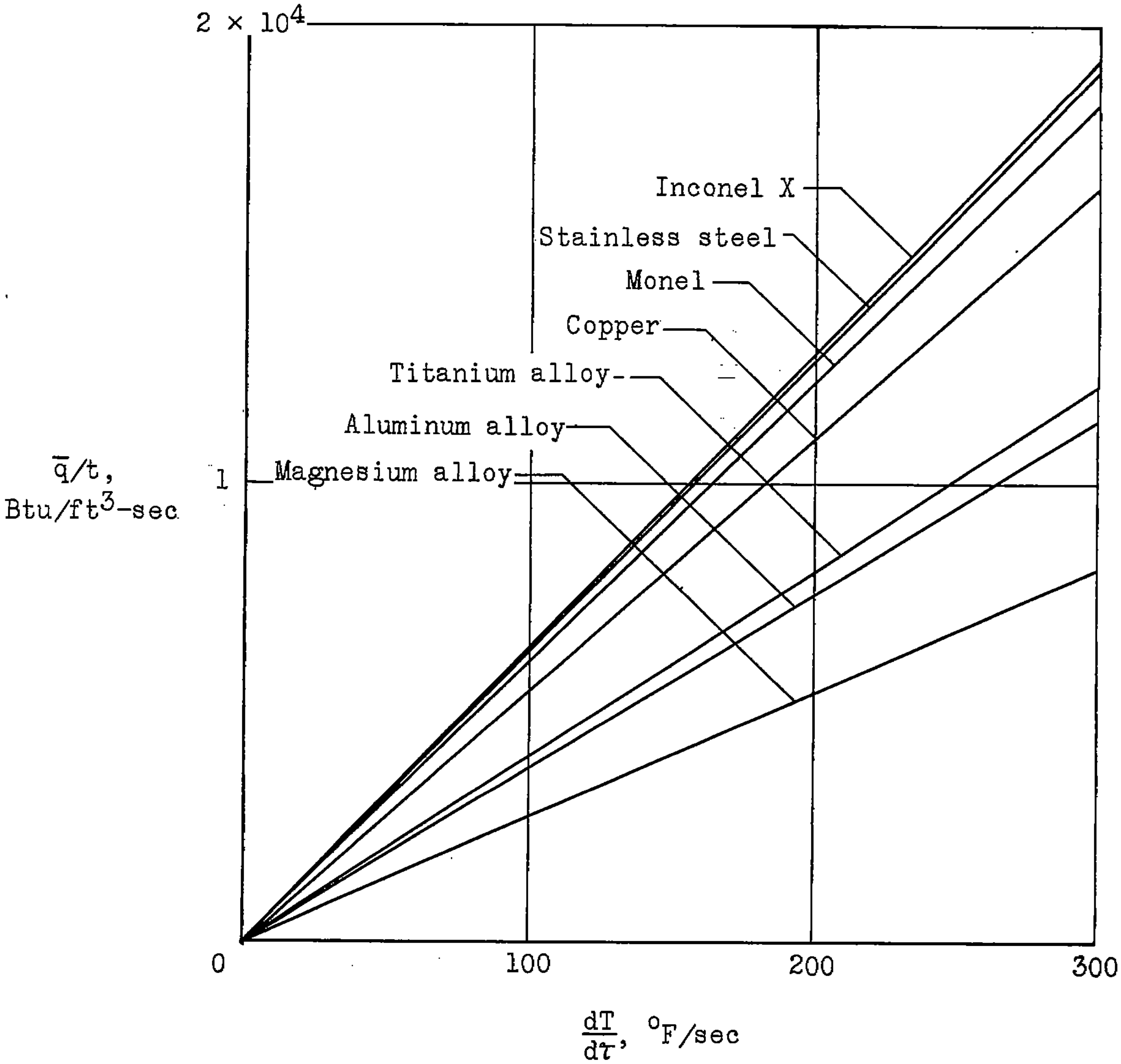

Figure 1.- Relation between heating rate and rate of temperature rise for thin plates of various materials. (See table I for material properties.)

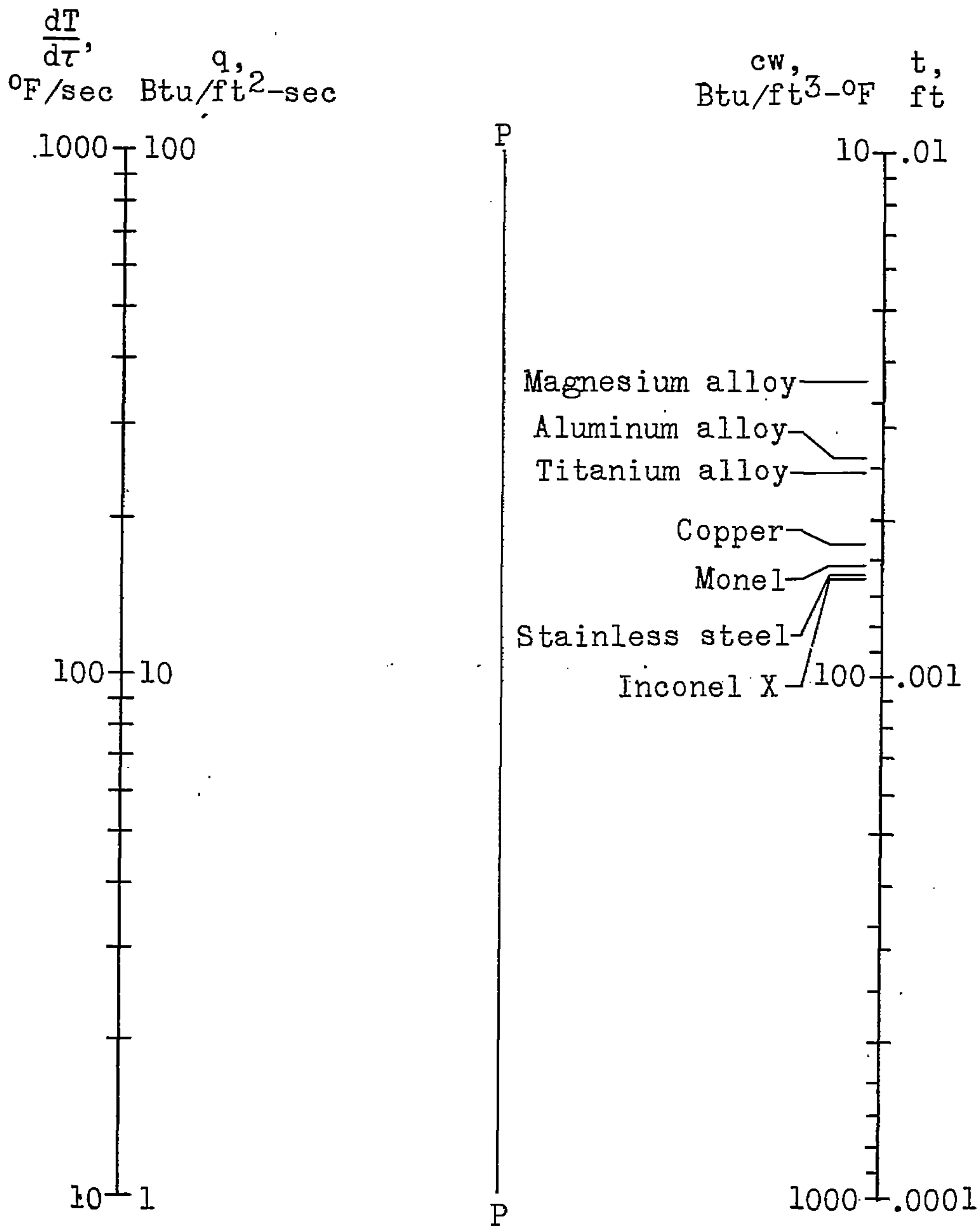

Key: The lines $\frac{dT}{d\tau}$-t and q-cw intersect on P-P.

Figure 2.- Nomograph for equation relating heating rate and rate of temperature rise in thin plate. $q = cwt \frac{dT}{d\tau}$.

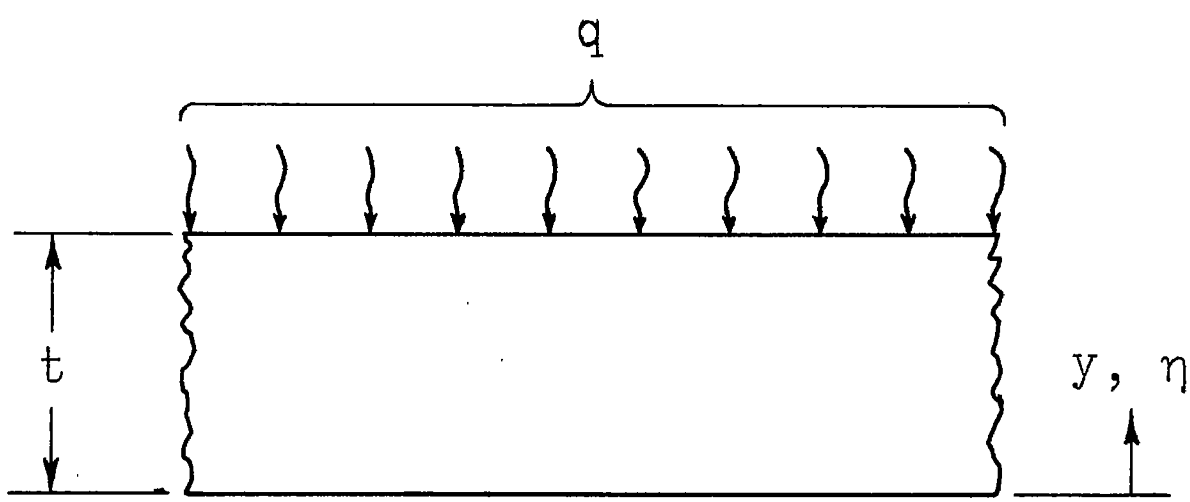

Figure 3.- Coordinate system for thick-plate analysis.

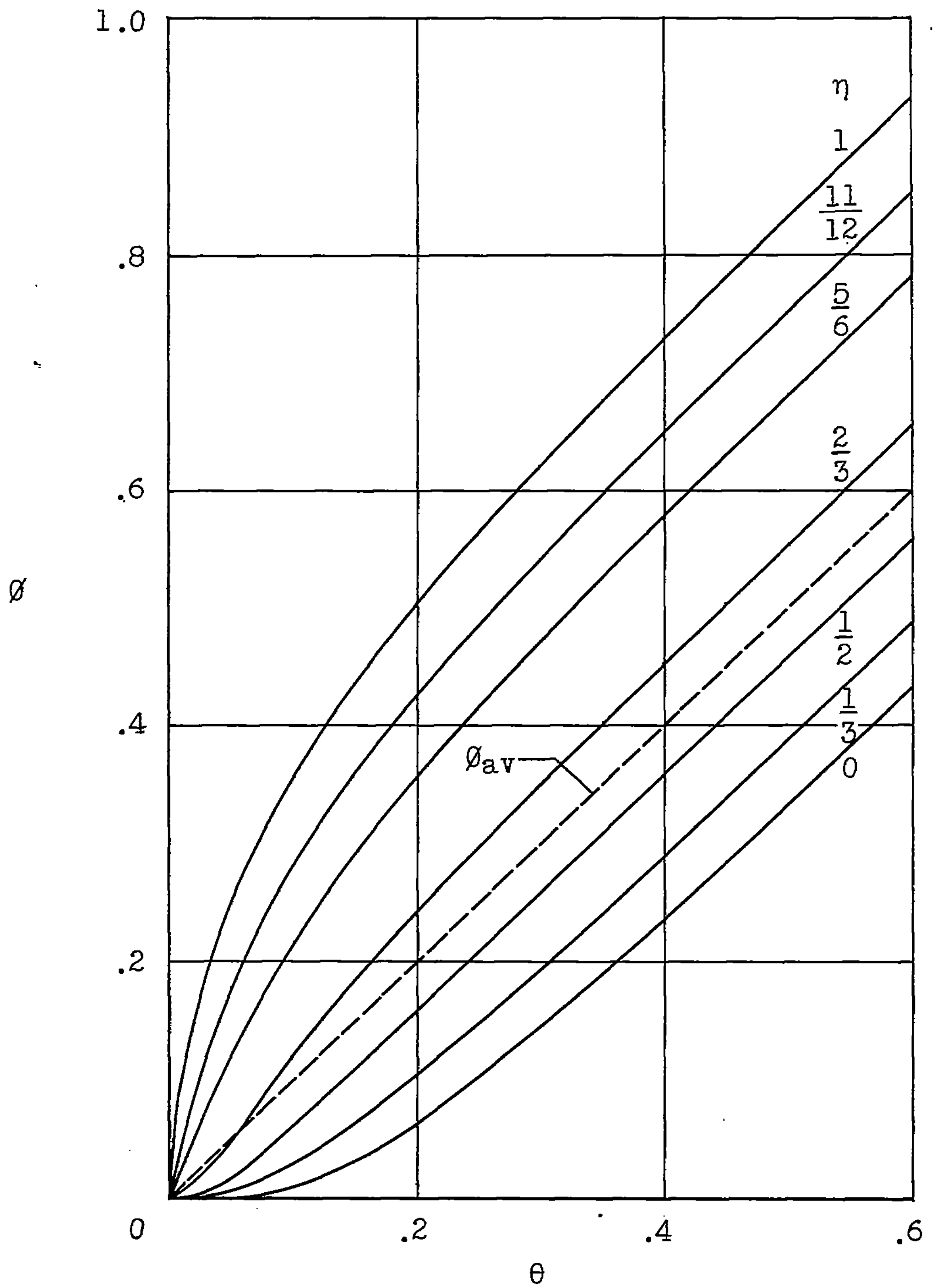

Figure 4.- Temperature history of thick plate subjected to constant heating rate.

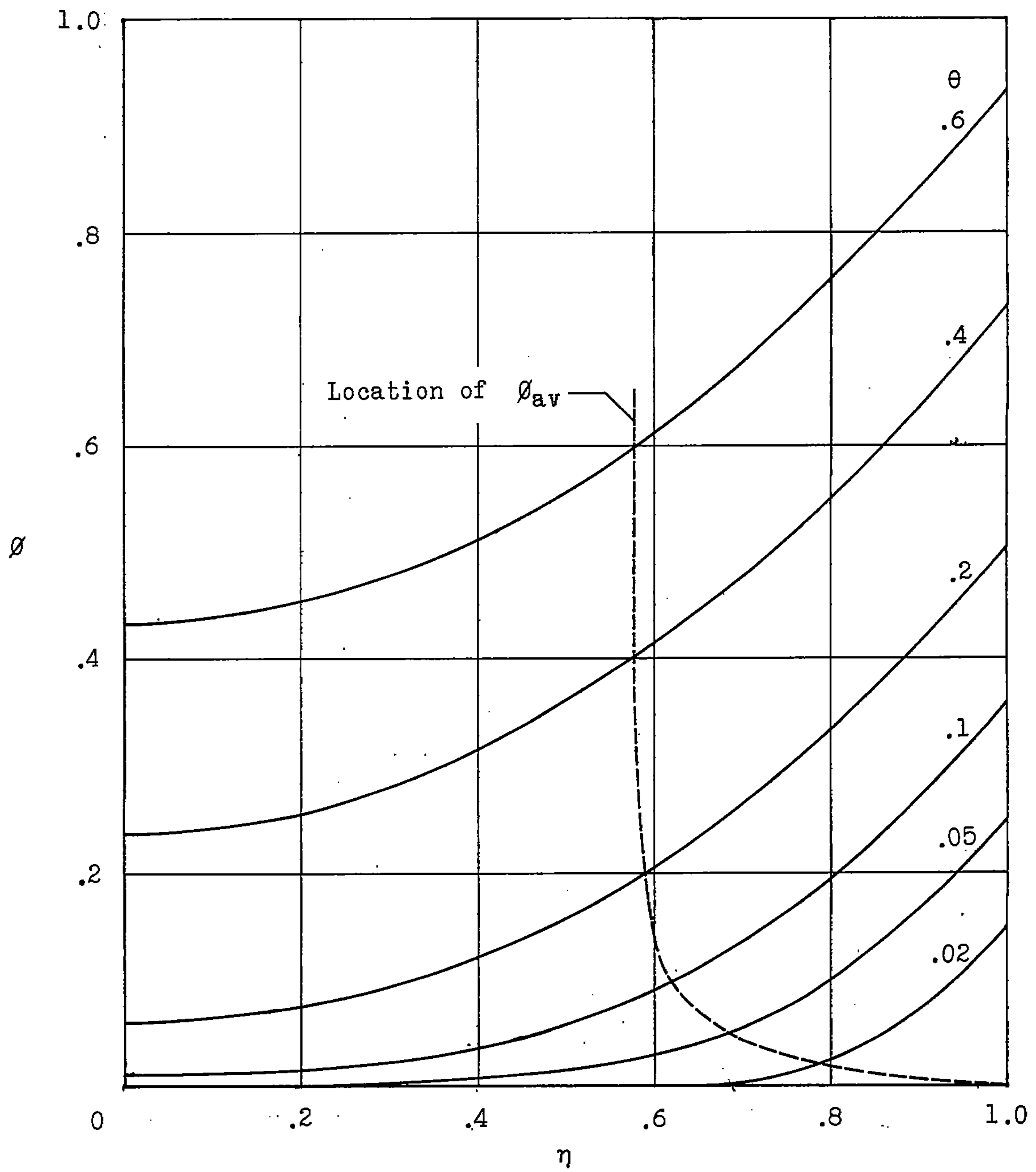

Figure 5.- Temperature distribution within thick plate subjected to constant heating rate.

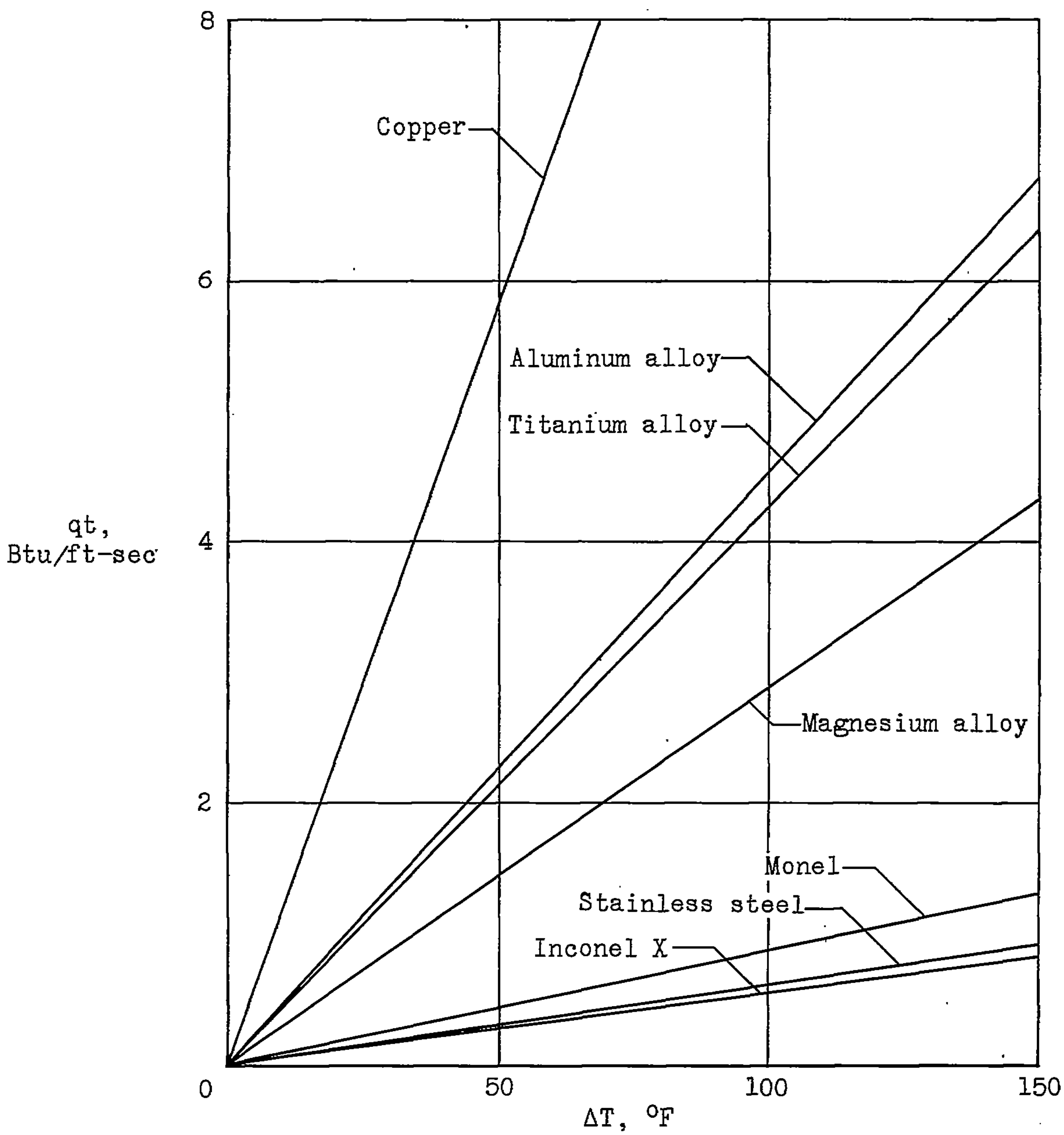

Figure 6.- Effect of constant heating rate on maximum temperature difference between heated and unheated surfaces of thick plates of various materials. (See table I for material properties.)

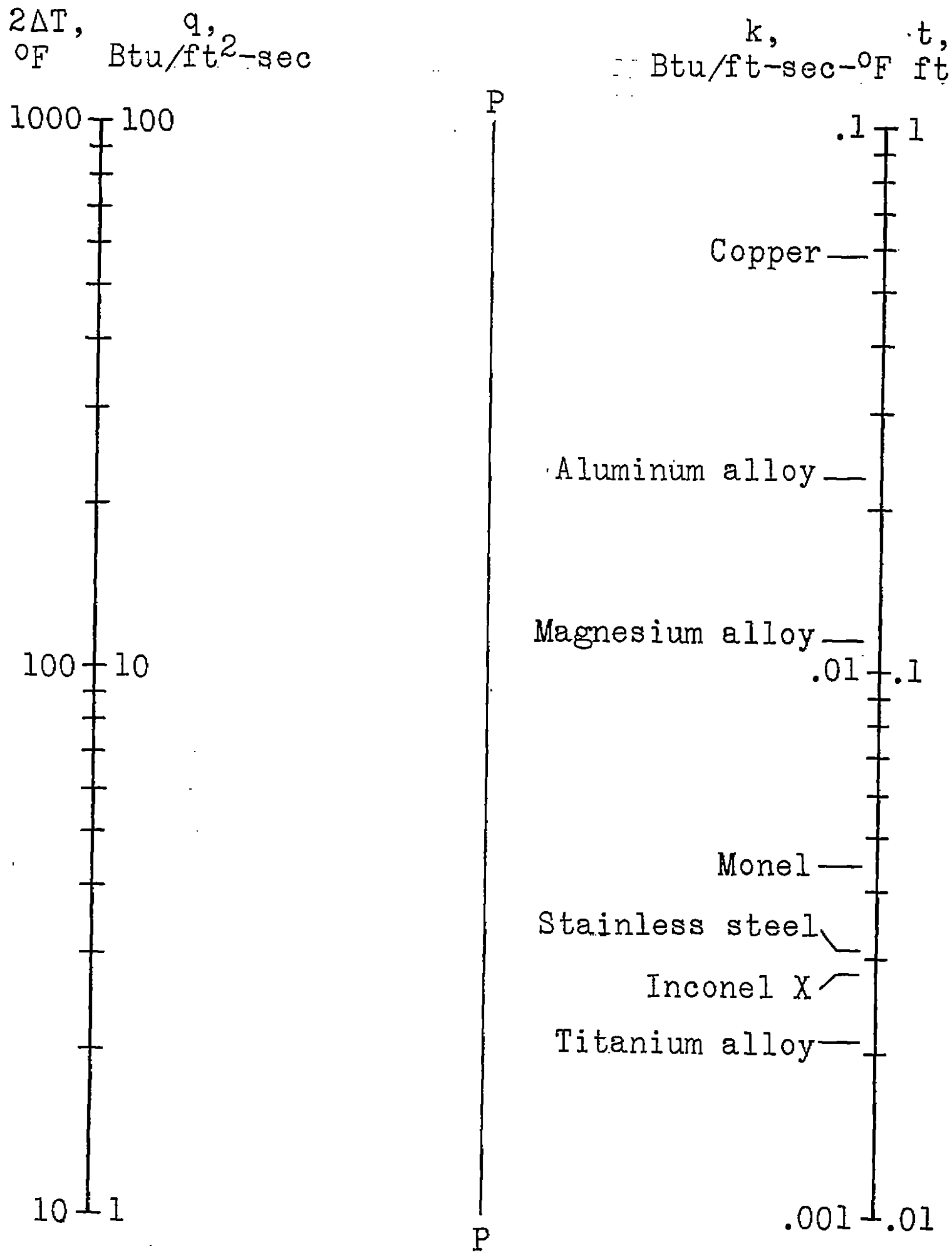

Key: The lines $2\Delta T$-k and q-t intersect on P-P.

Figure 7.- Nomograph for equation relating heating rate and maximum temperature difference through thick plate. $\Delta T = \frac{1}{2}\frac{qt}{k}$.

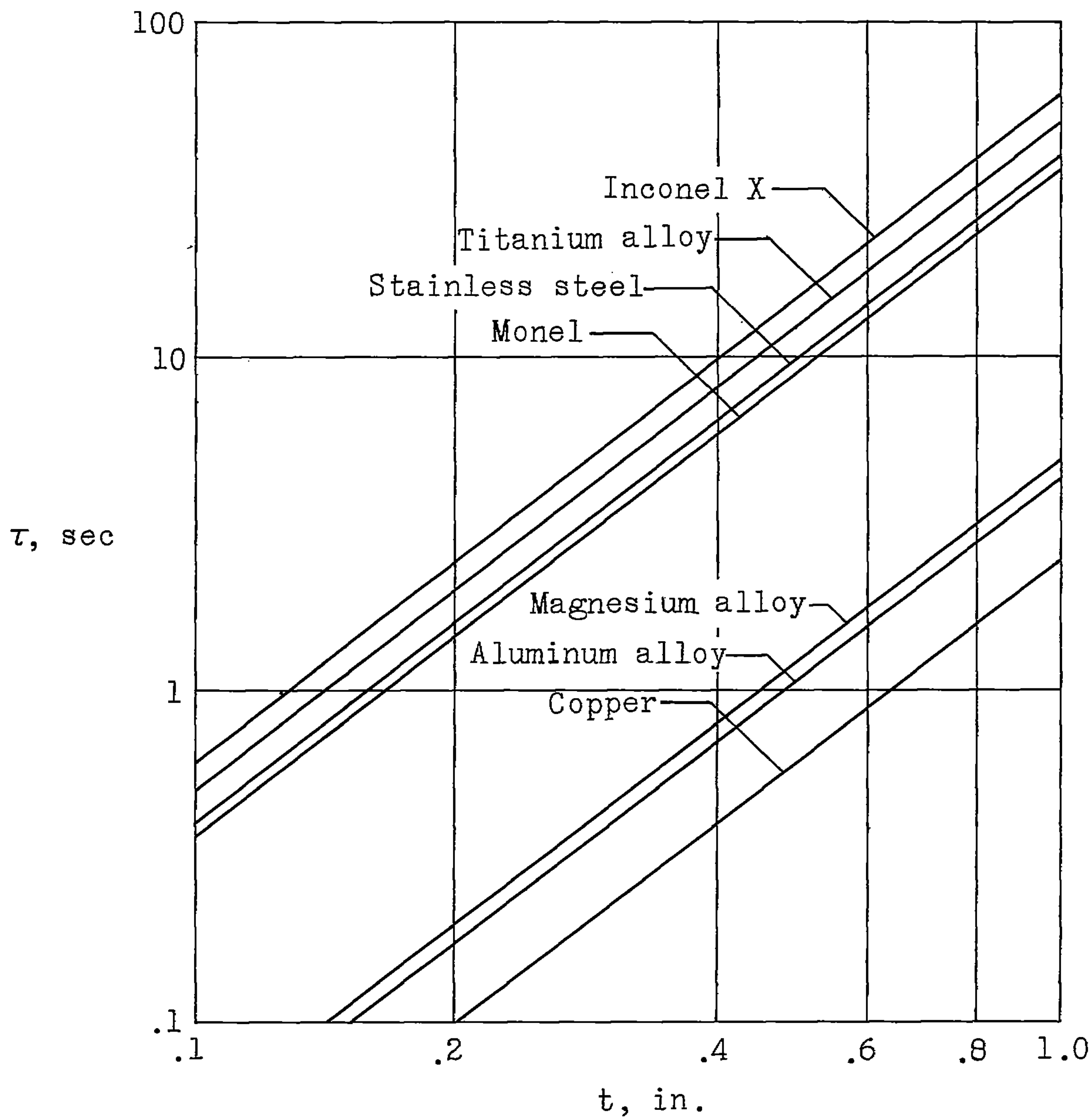

Figure 8.- Time required to produce 98 percent of maximum temperature difference between heated and unheated surfaces of thick plates of various materials subjected to constant heating rate. (See table I for material properties.)

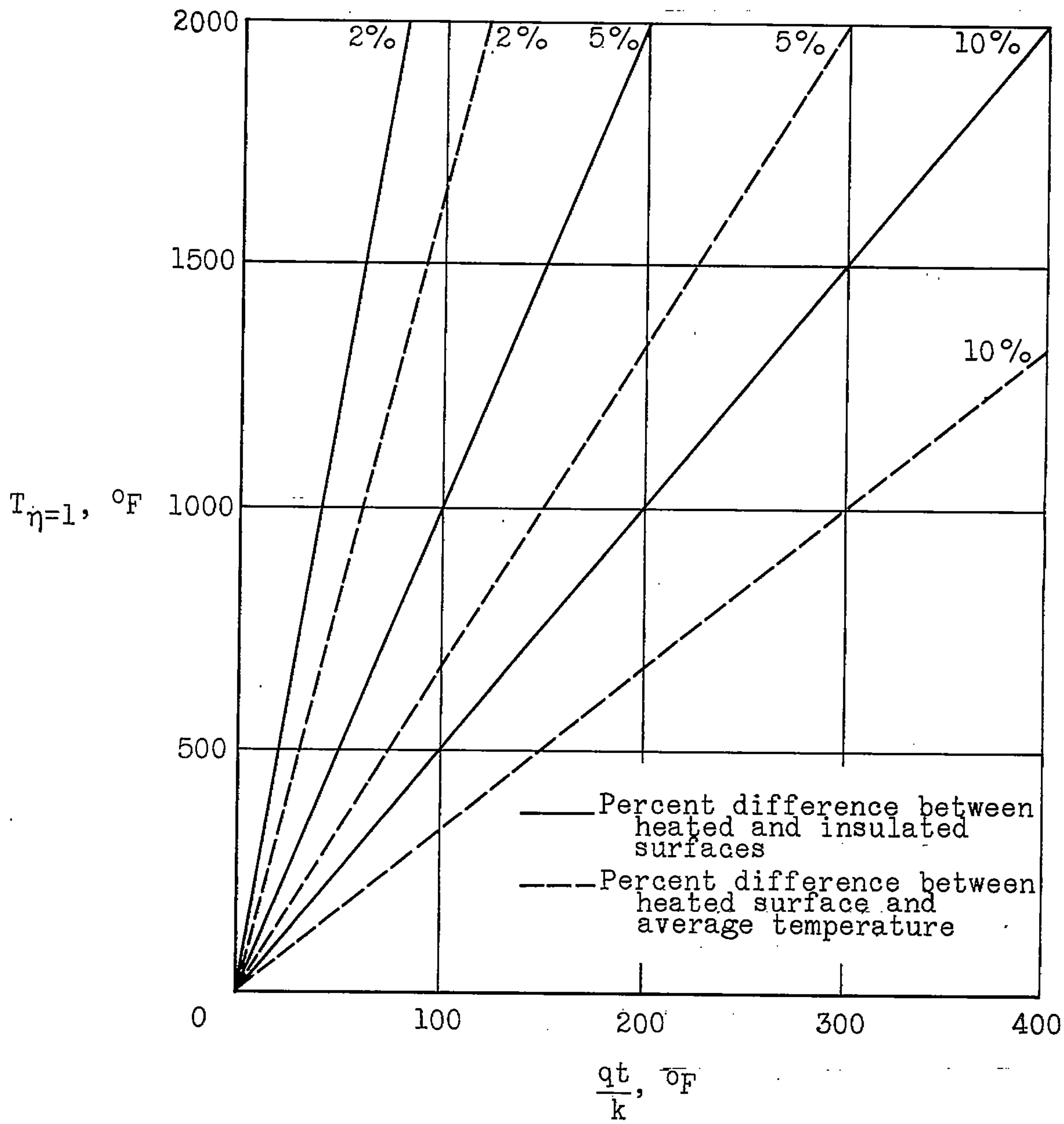

Figure 9.- Assigned temperature differences as function of temperature of heated surface of plate and heating rate.

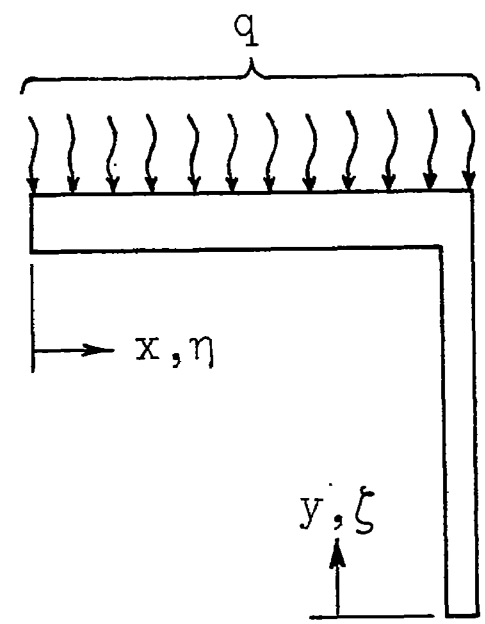

(a) Basic angle section.

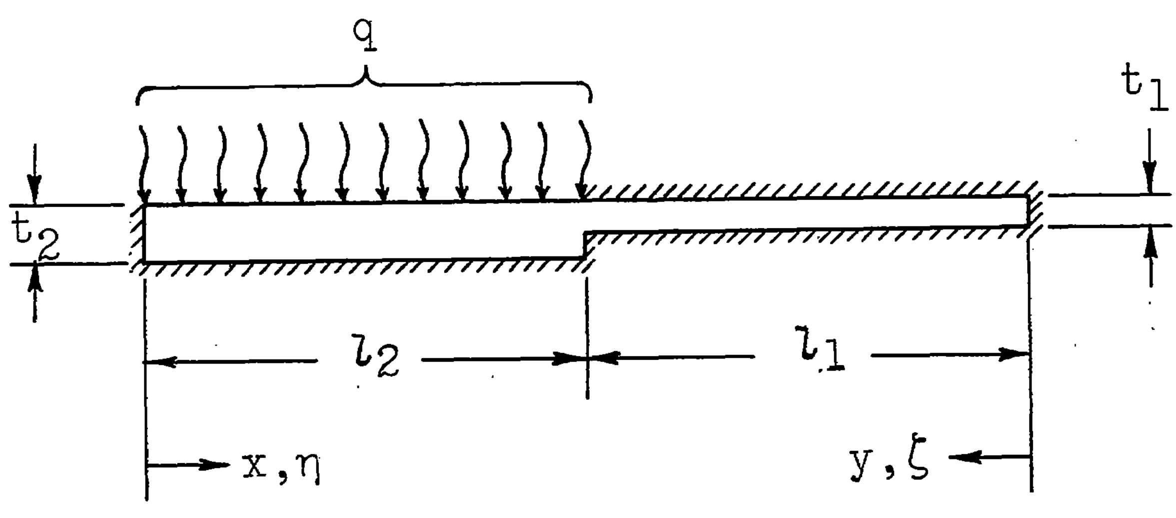

(b) Idealized angle section.

Figure 10.- Angle section employed to investigate temperature and thermal stress distributions in various structural shapes.

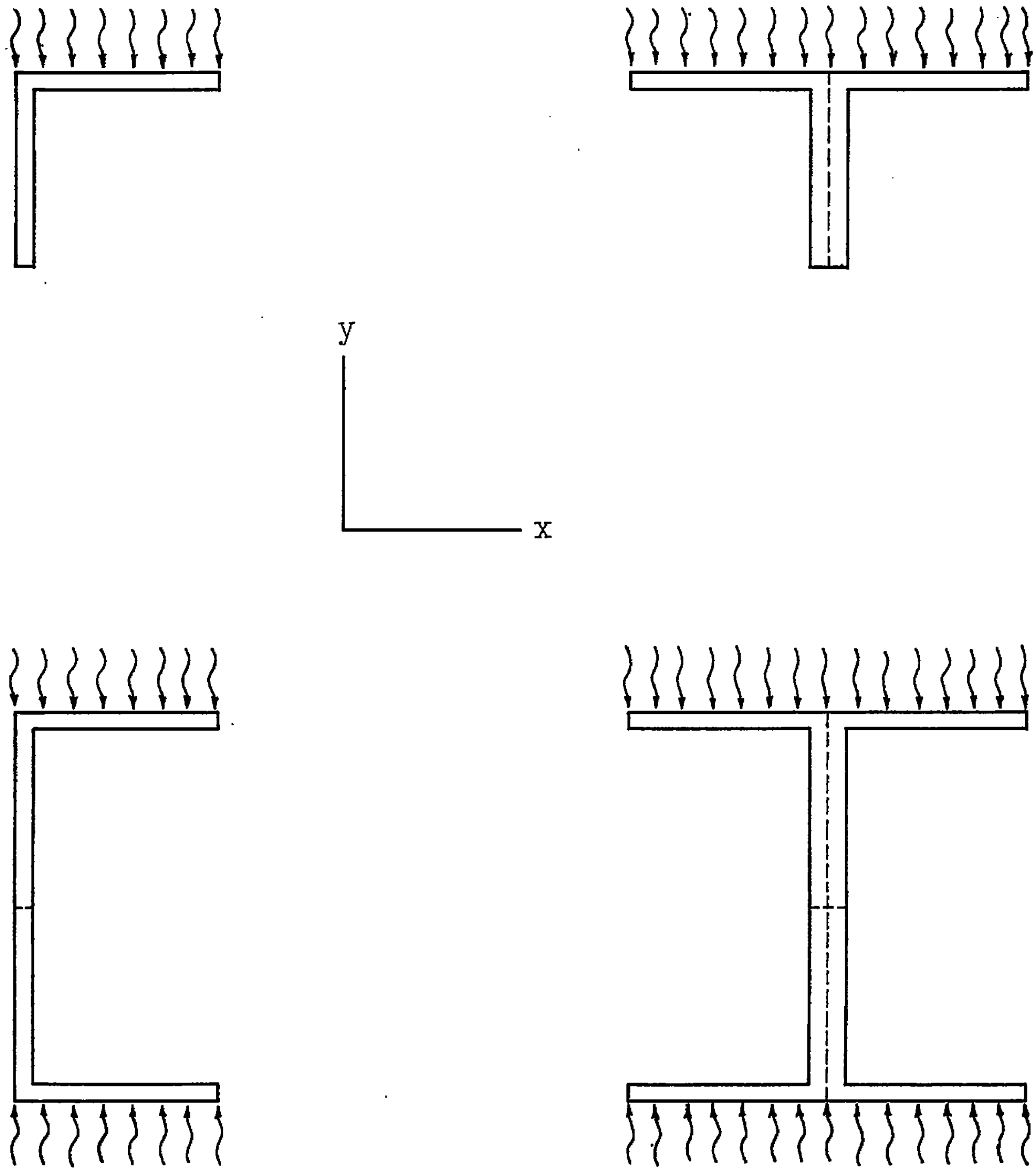

Figure 11.- Structural shapes formed by combinations of angle sections.

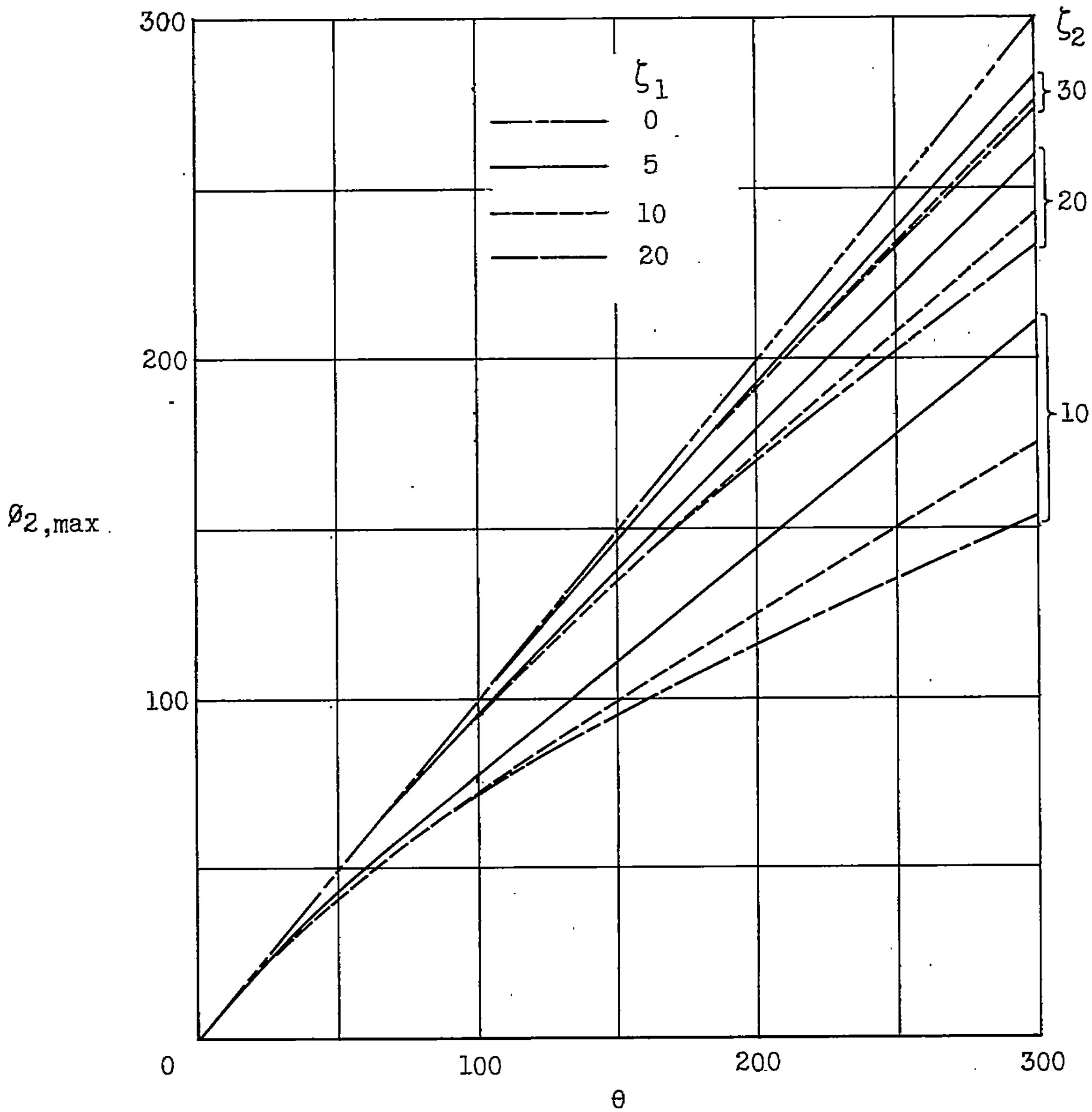

(a) $\frac{t_2}{t_1} = 1.$

Figure 12.- History of maximum temperature of angle section for various proportions.

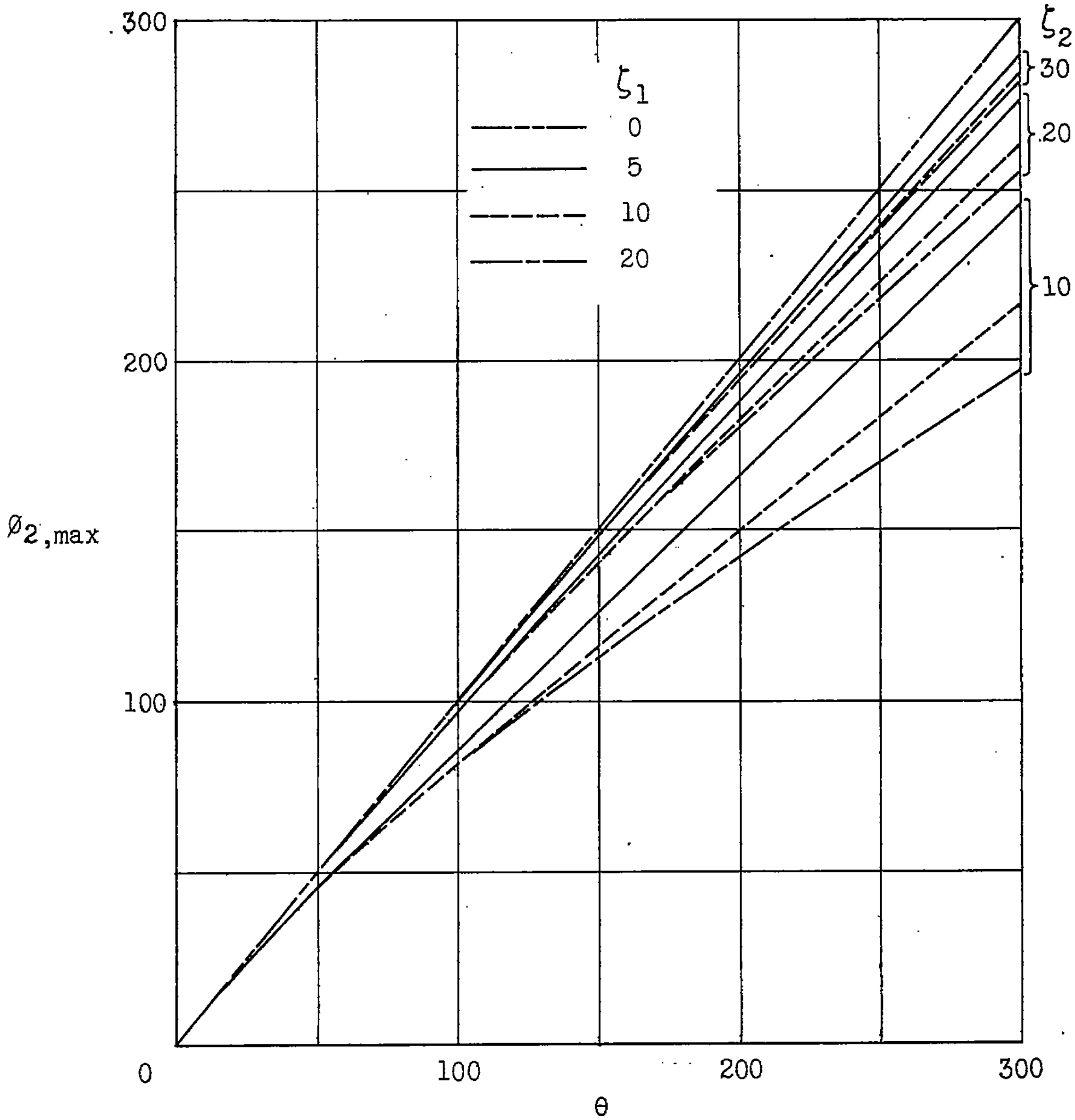

(b) $\frac{t_2}{t_1} = 2.$

Figure 12.- Continued.

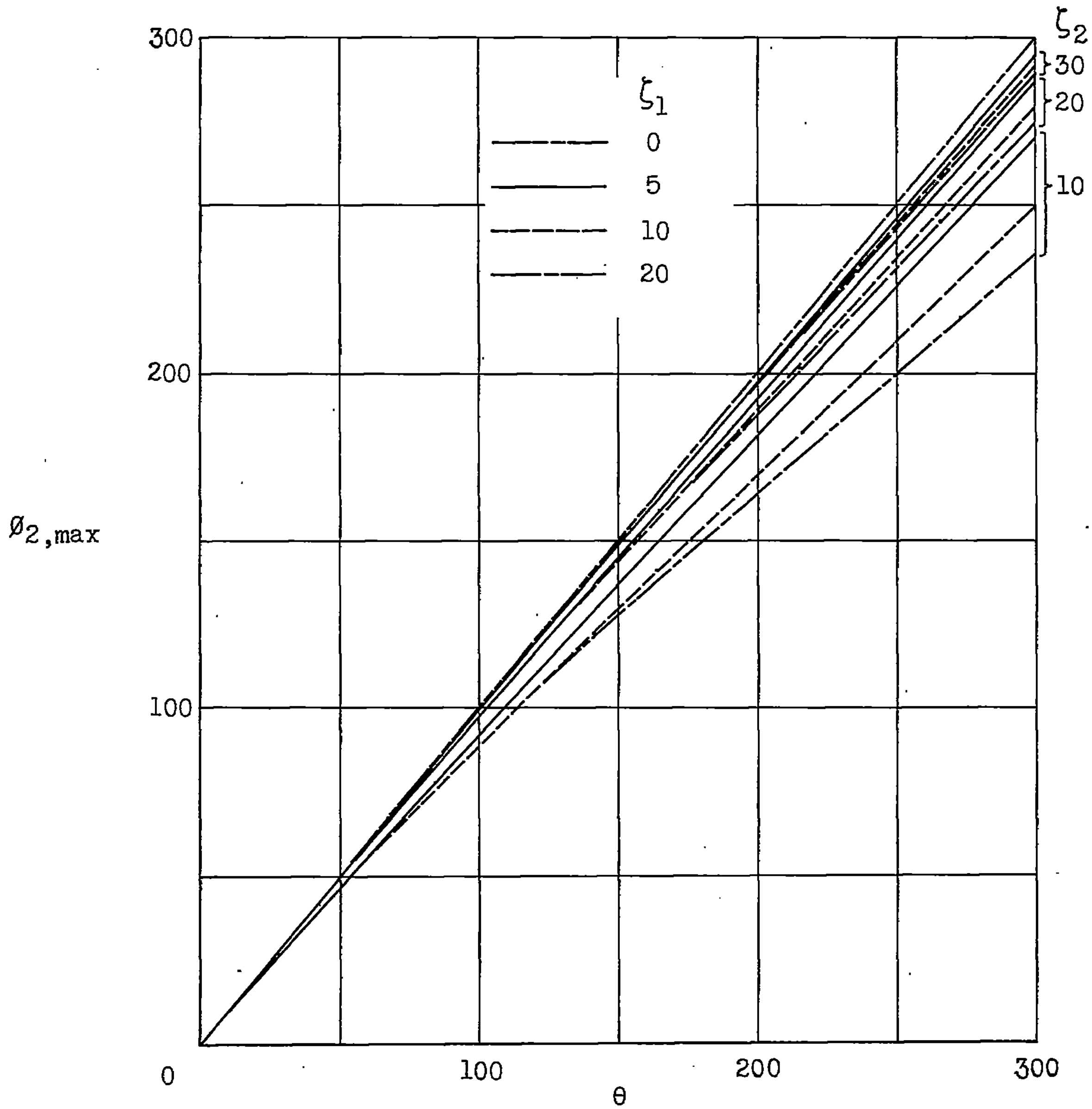

(c) $\frac{t_2}{t_1} = 4.$

Figure 12.- Concluded.

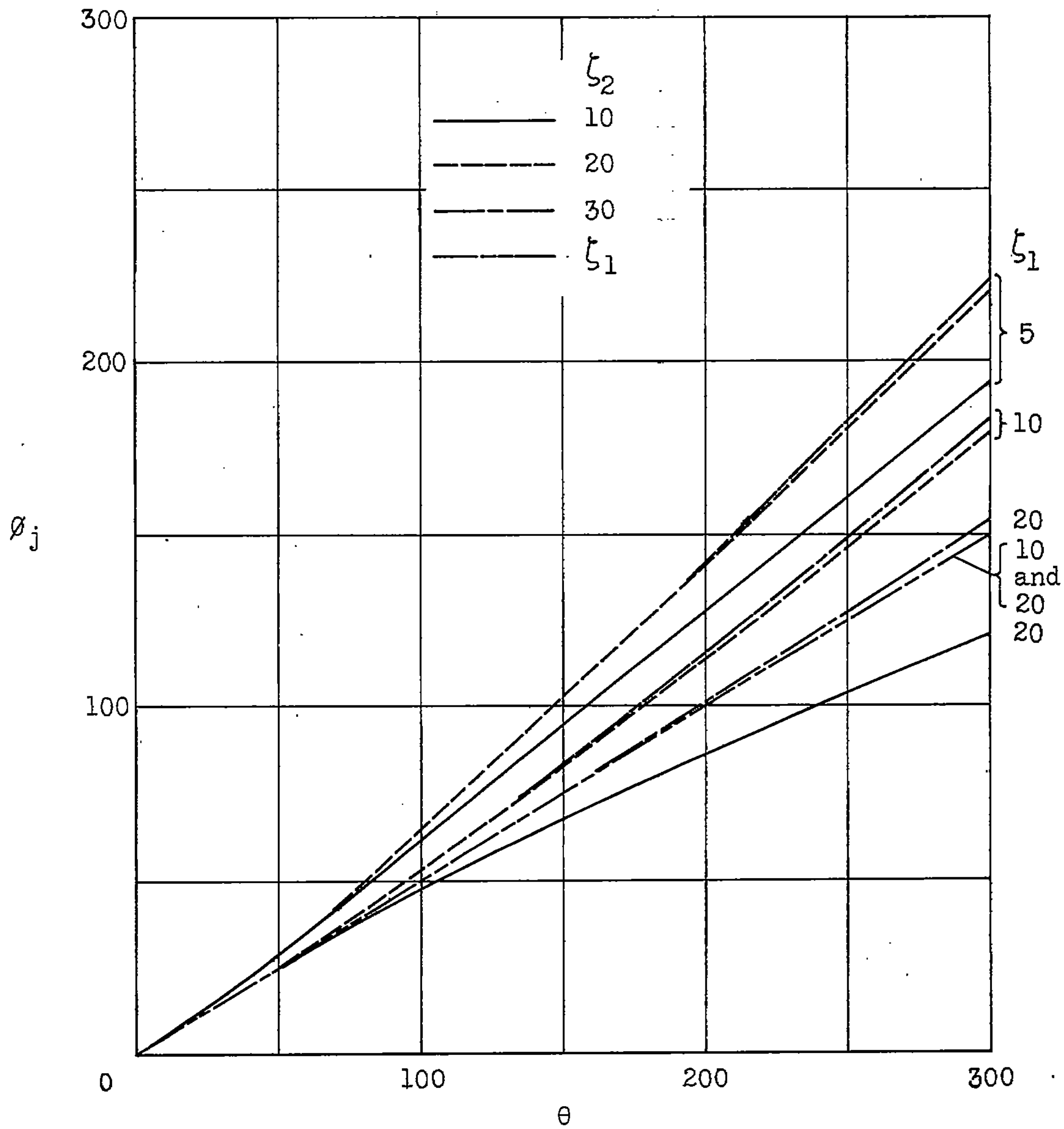

(a) $\frac{t_2}{t_1} = 1$.

Figure 13.- History of temperature at junction of elements of angle section for various proportions.

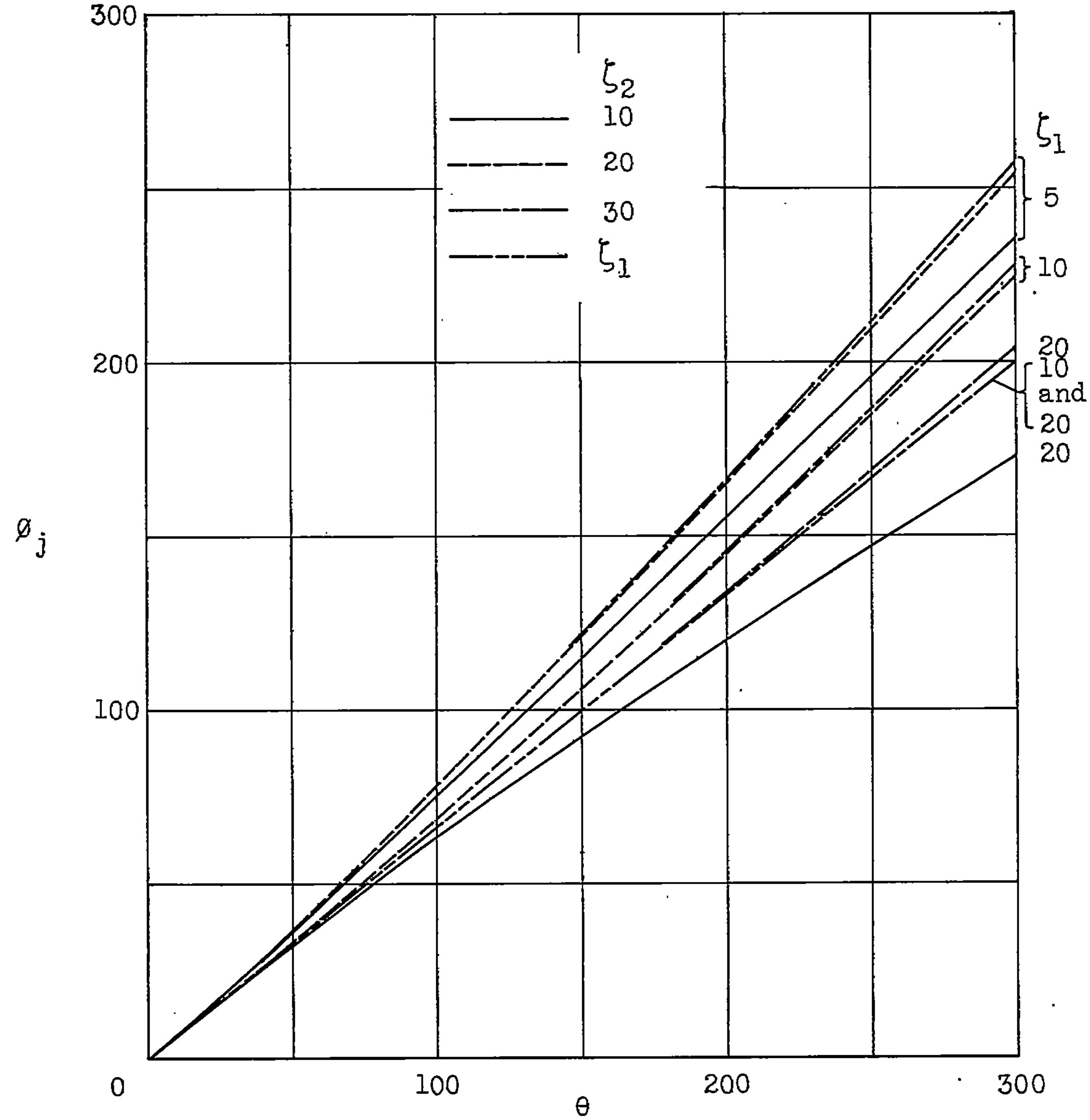

(b) $\frac{t_2}{t_1} = 2.$

Figure 13.- Continued.

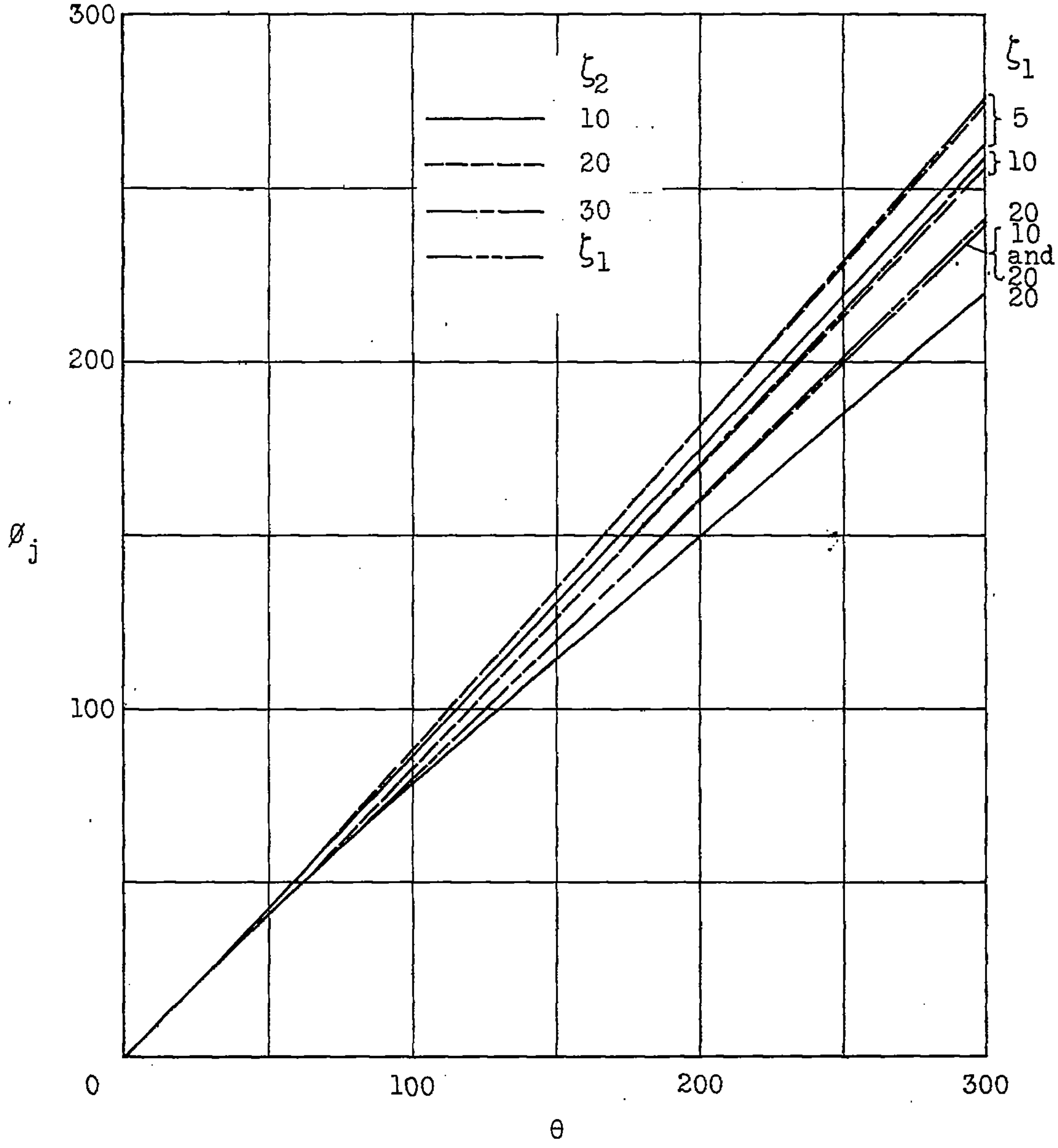

(c) $\frac{t_2}{t_1} = 4.$

Figure 13.- Concluded.

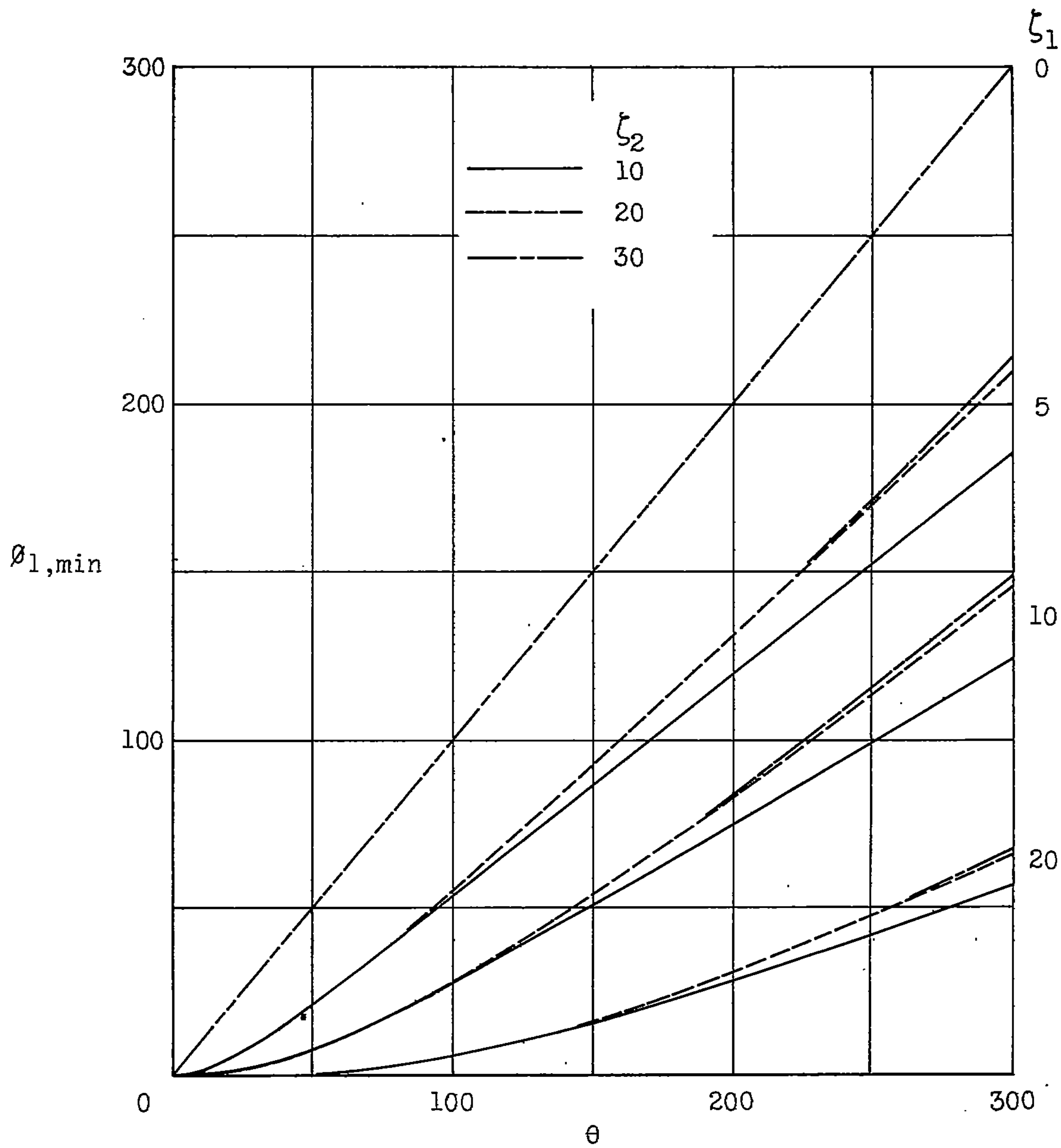

(a) $\frac{t_2}{t_1} = 1.$

Figure 14.- History of minimum temperature of angle section for various proportions.

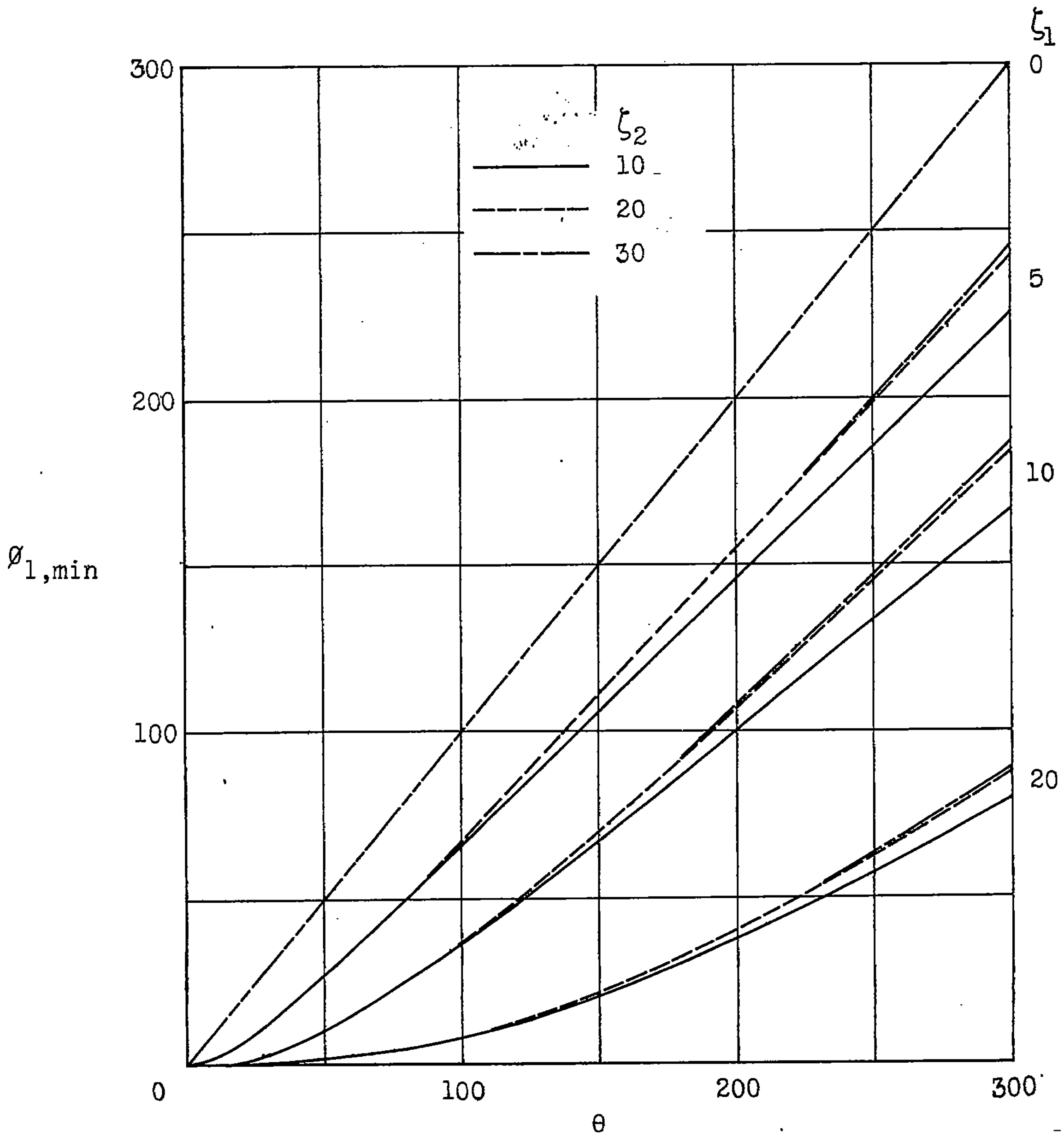

(b) $\frac{t_2}{t_1} = 2.$

Figure 14.- Continued.

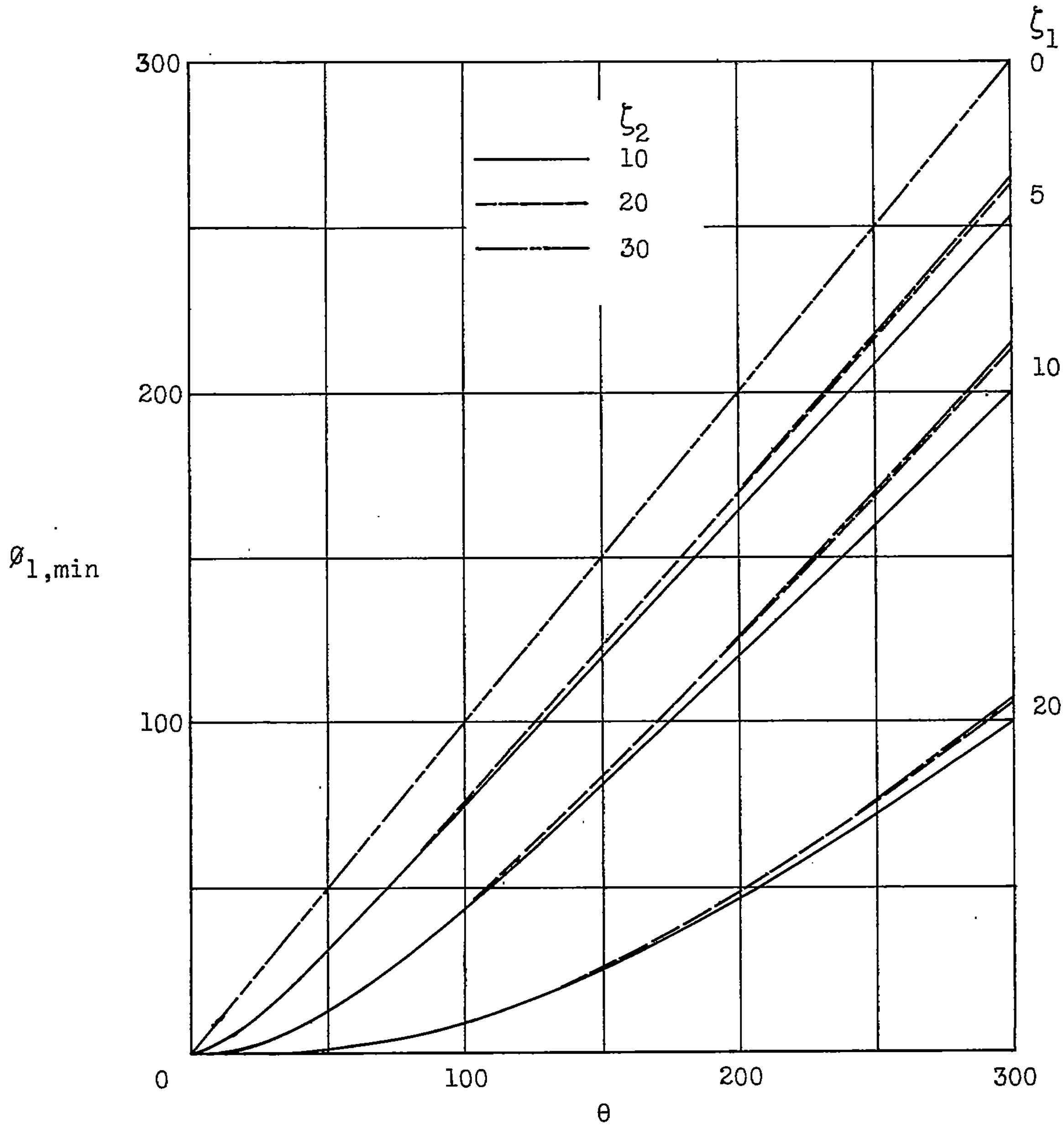

(c) $\frac{t_2}{t_1} = 4$.

Figure 14.- Concluded.

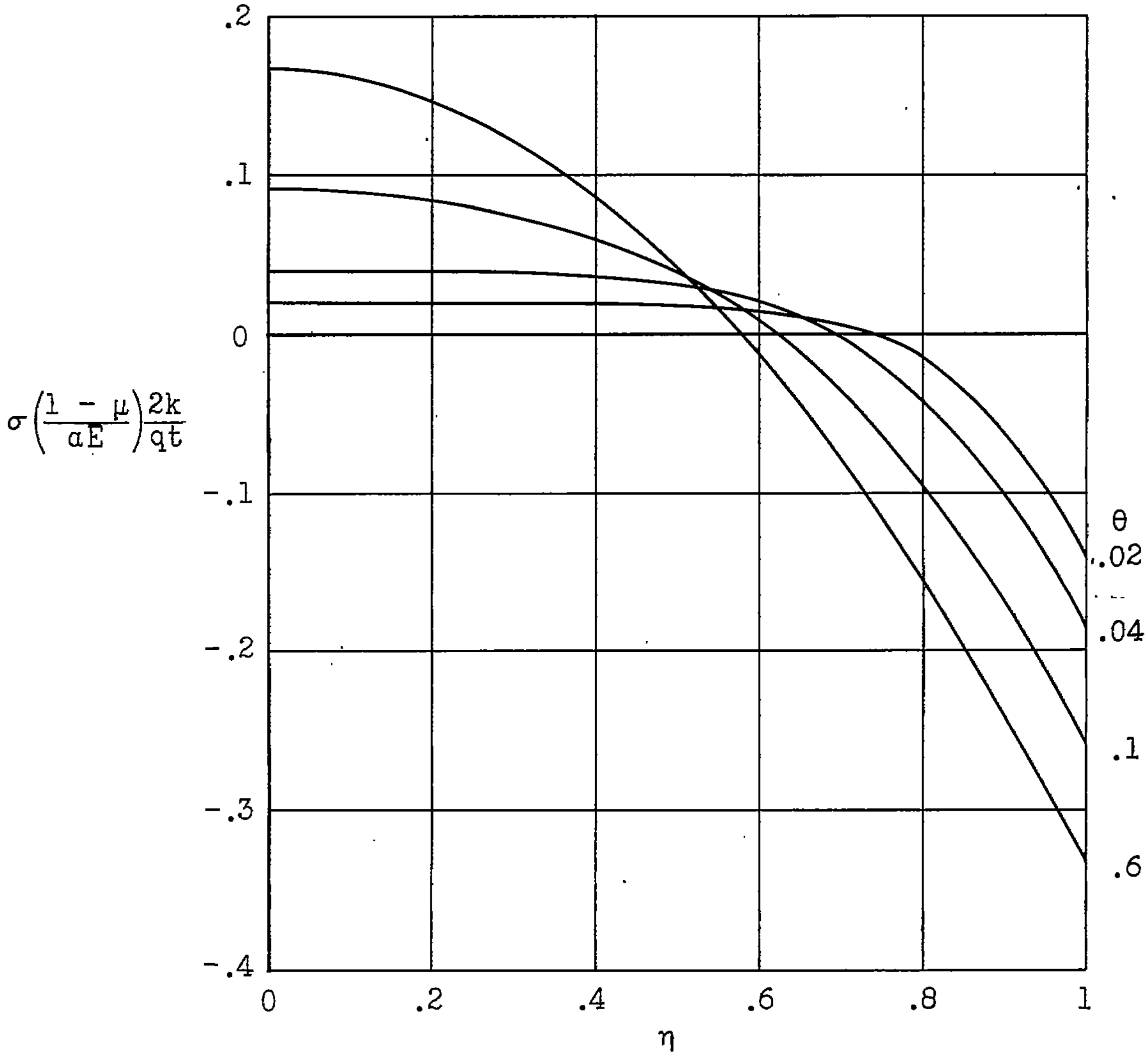

Figure 15.- Thermal stress distribution in symmetrically heated thick plate subjected to constant heating rate.

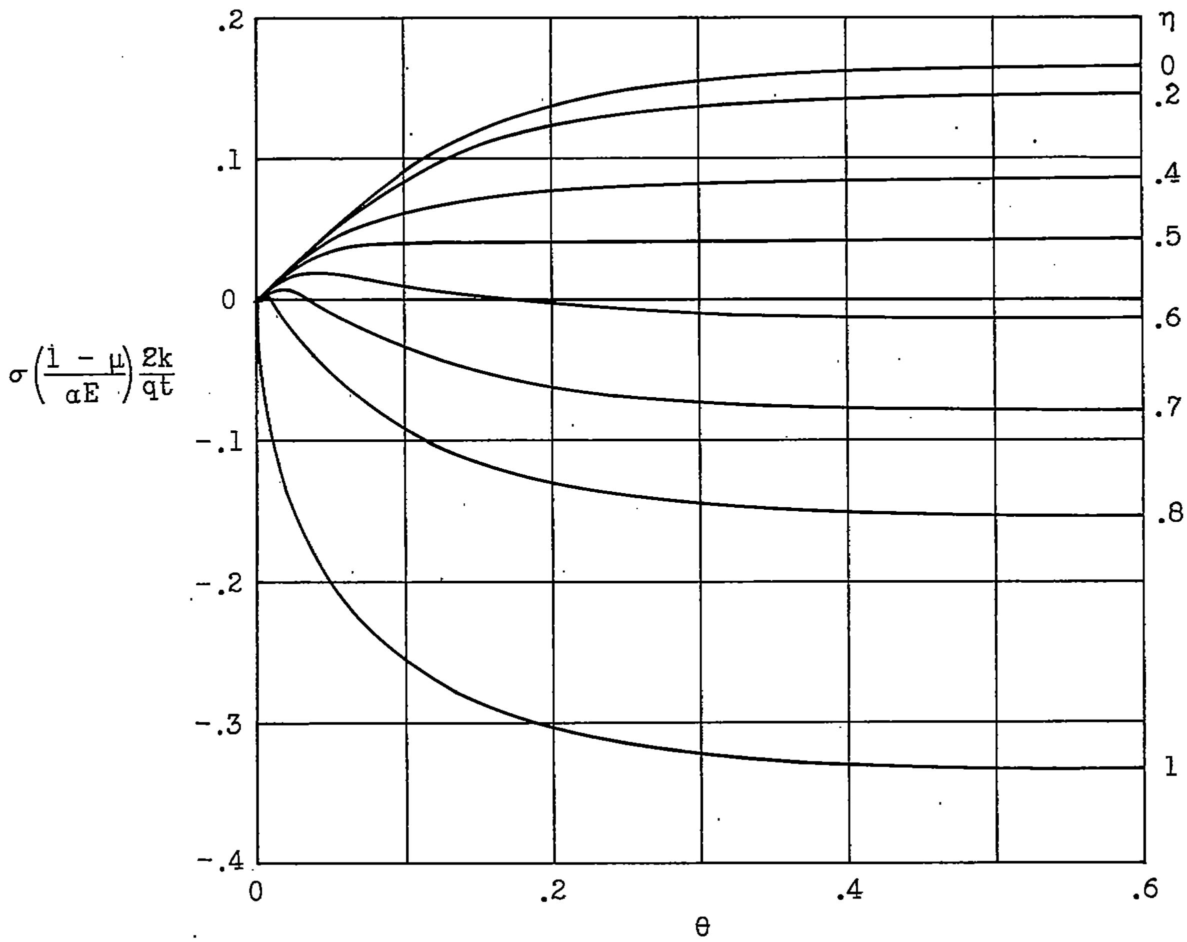

Figure 16.- History of stresses in symmetrically heated thick plate subjected to constant heating rate.

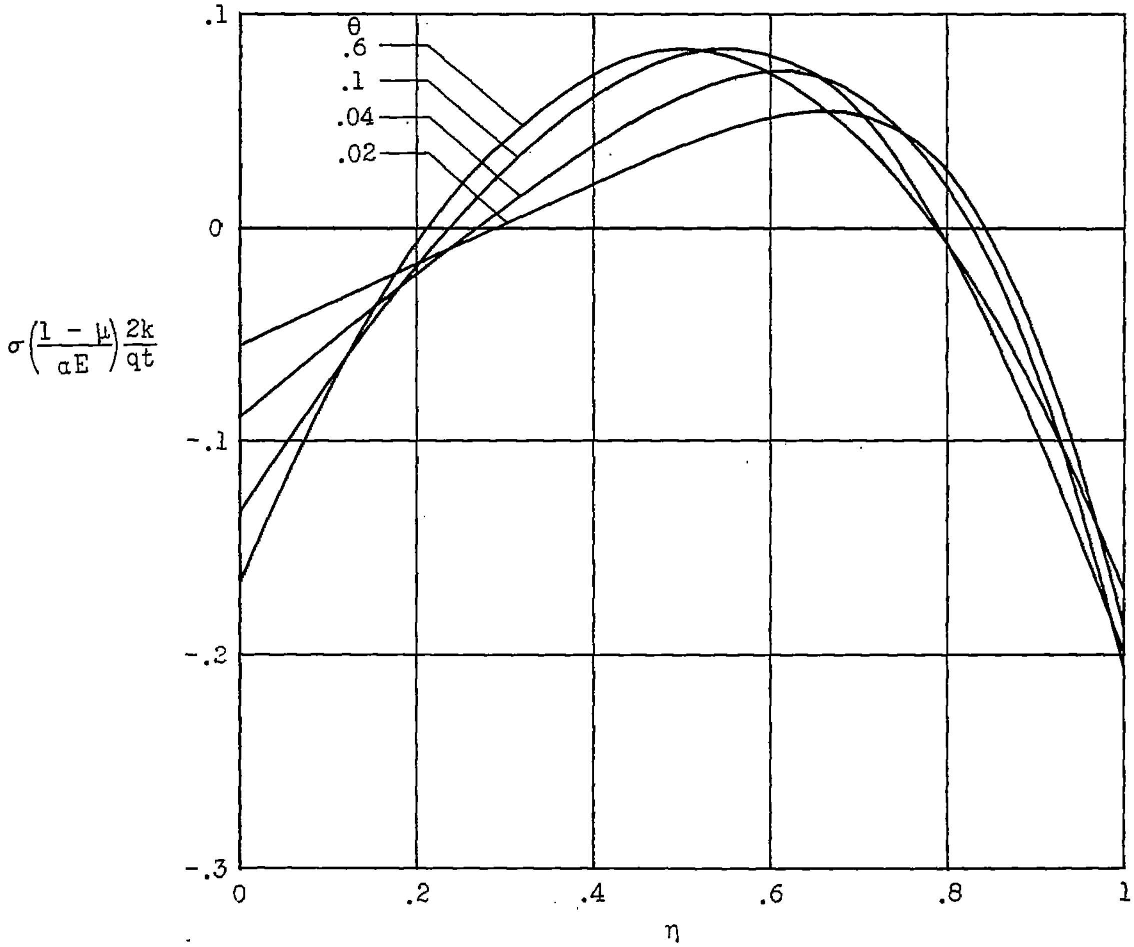

Figure 17.- Stress distribution in thick plate subjected to constant heating rate on one surface.

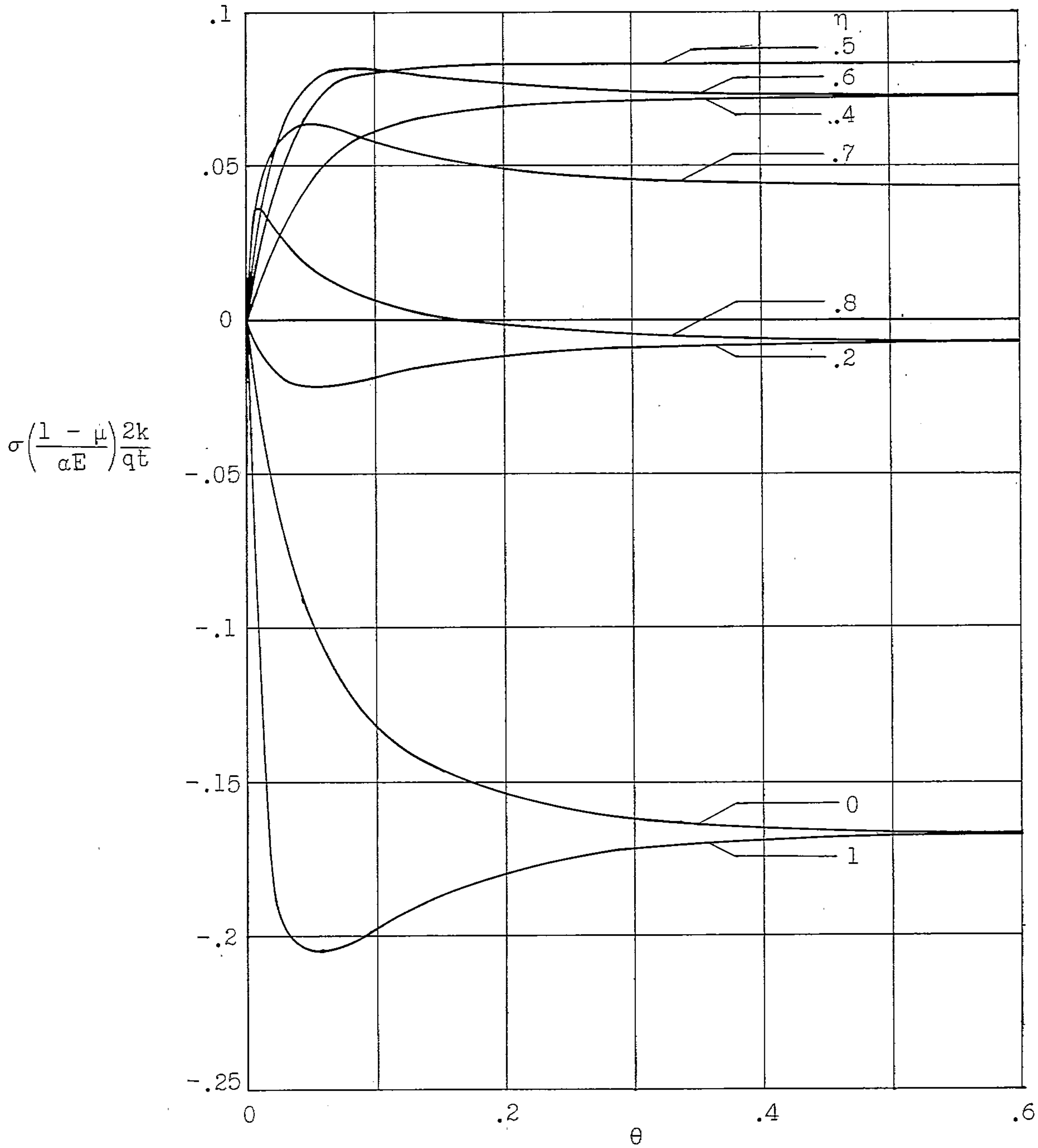

Figure 18.- History of stresses in thick plate subjected to constant heating rate on one surface.

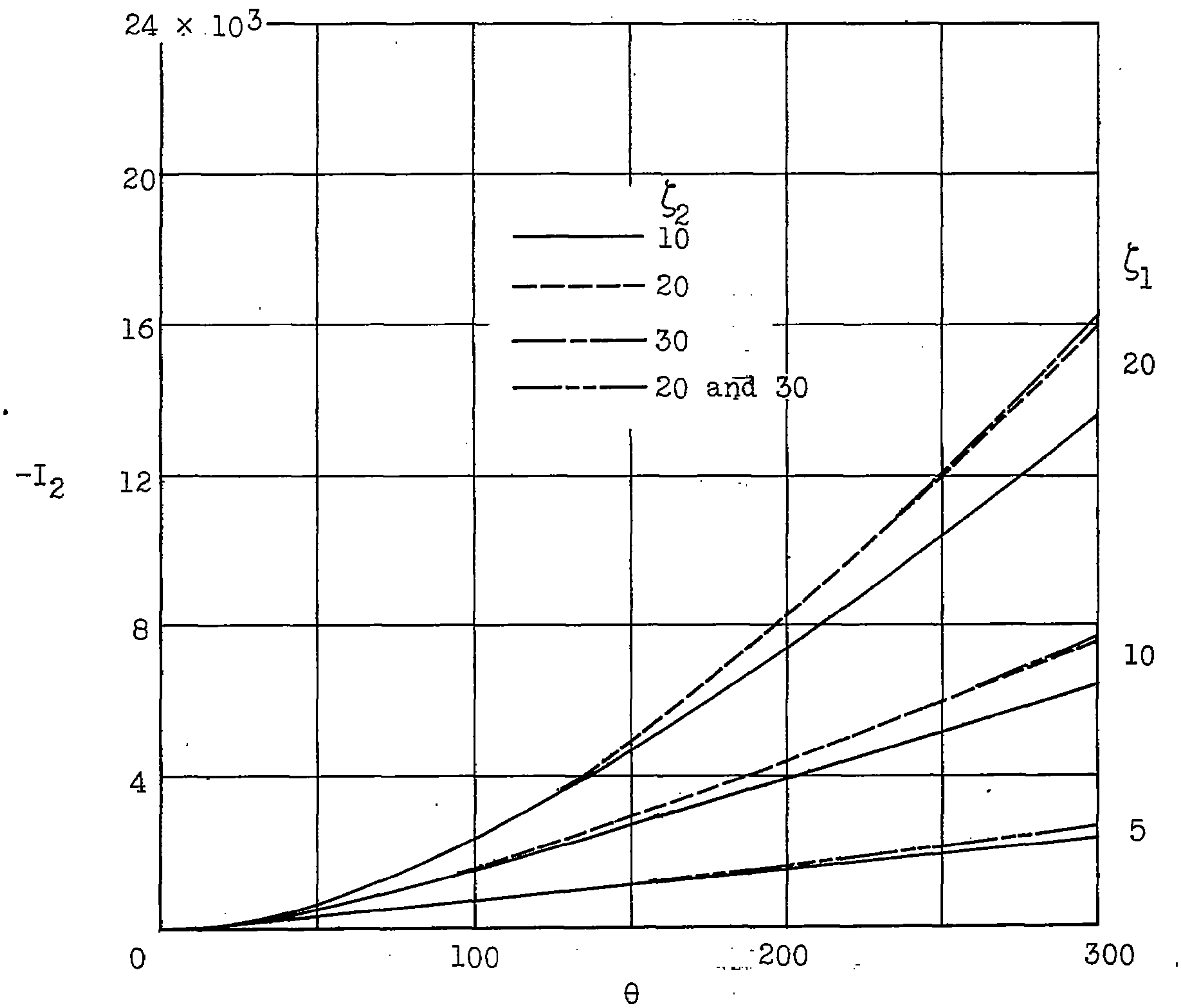

(a) $\frac{t_2}{t_1} = 1.$

Figure 19.- Values of function I_2 appearing in stress equations for angle, channel, and T-sections.

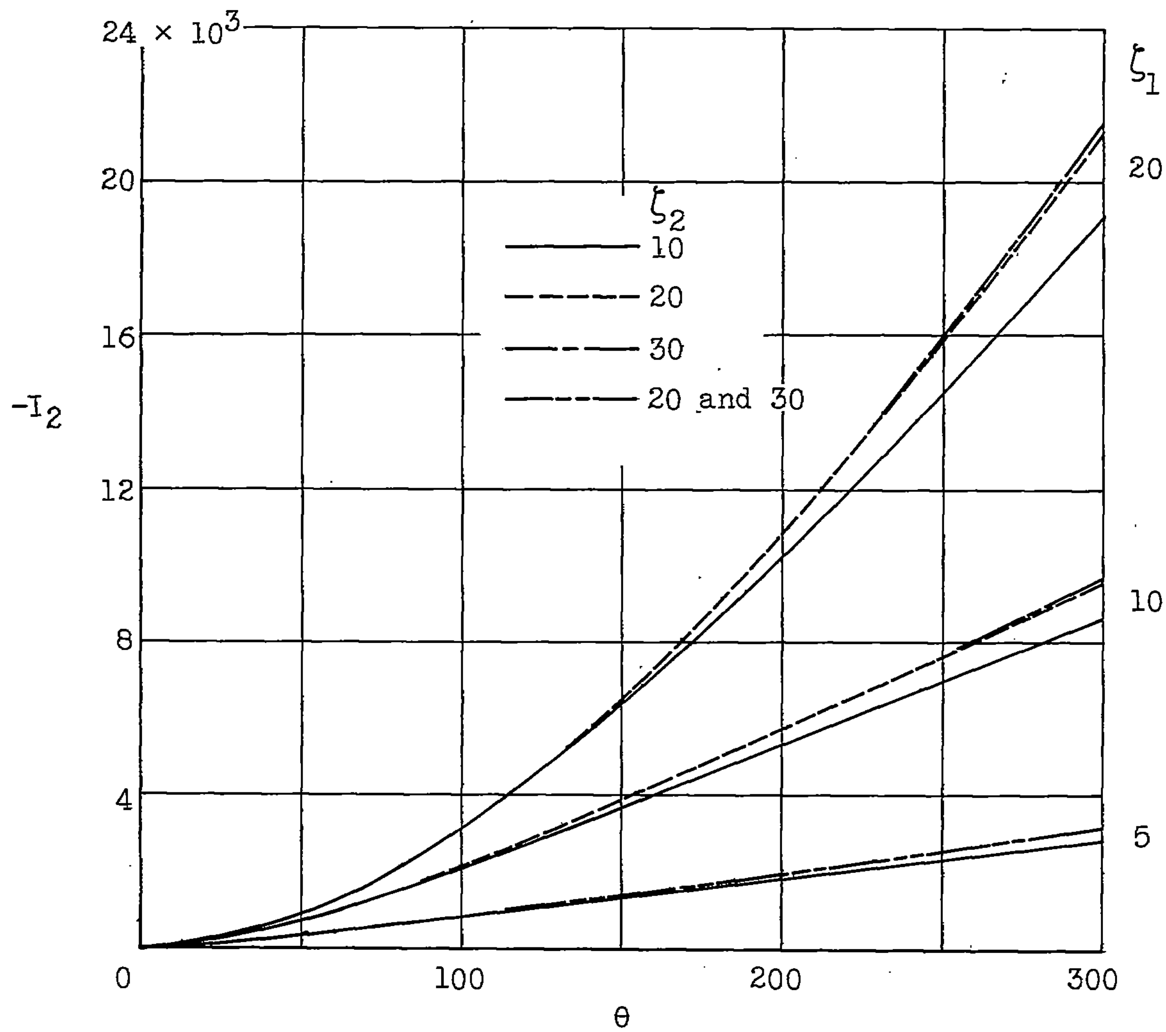

(b) $\frac{t_2}{t_1} = 2.$

Figure 19.- Continued.

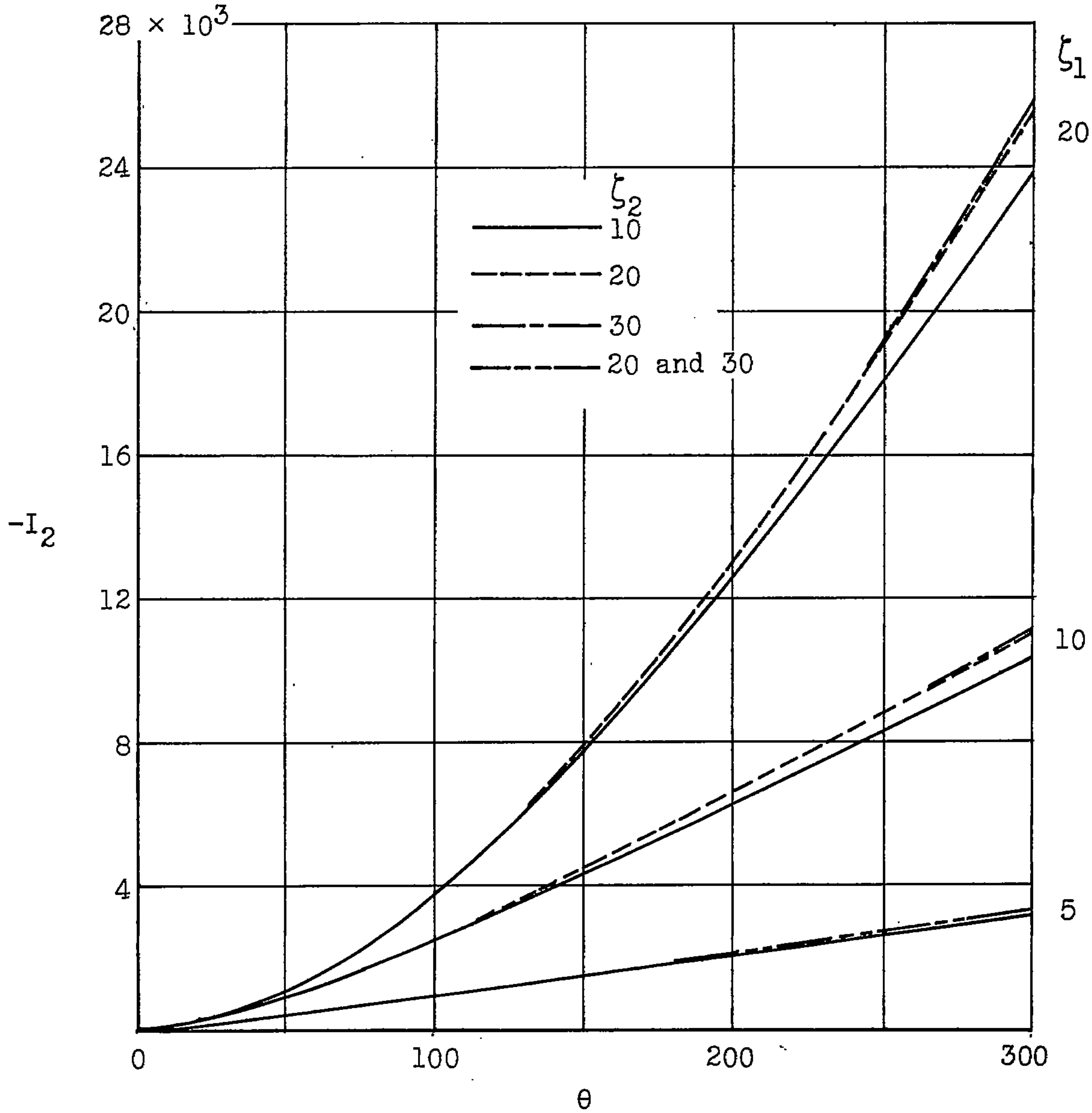

(c) $\frac{t_2}{t_1} = 4.$

Figure 19.- Concluded.

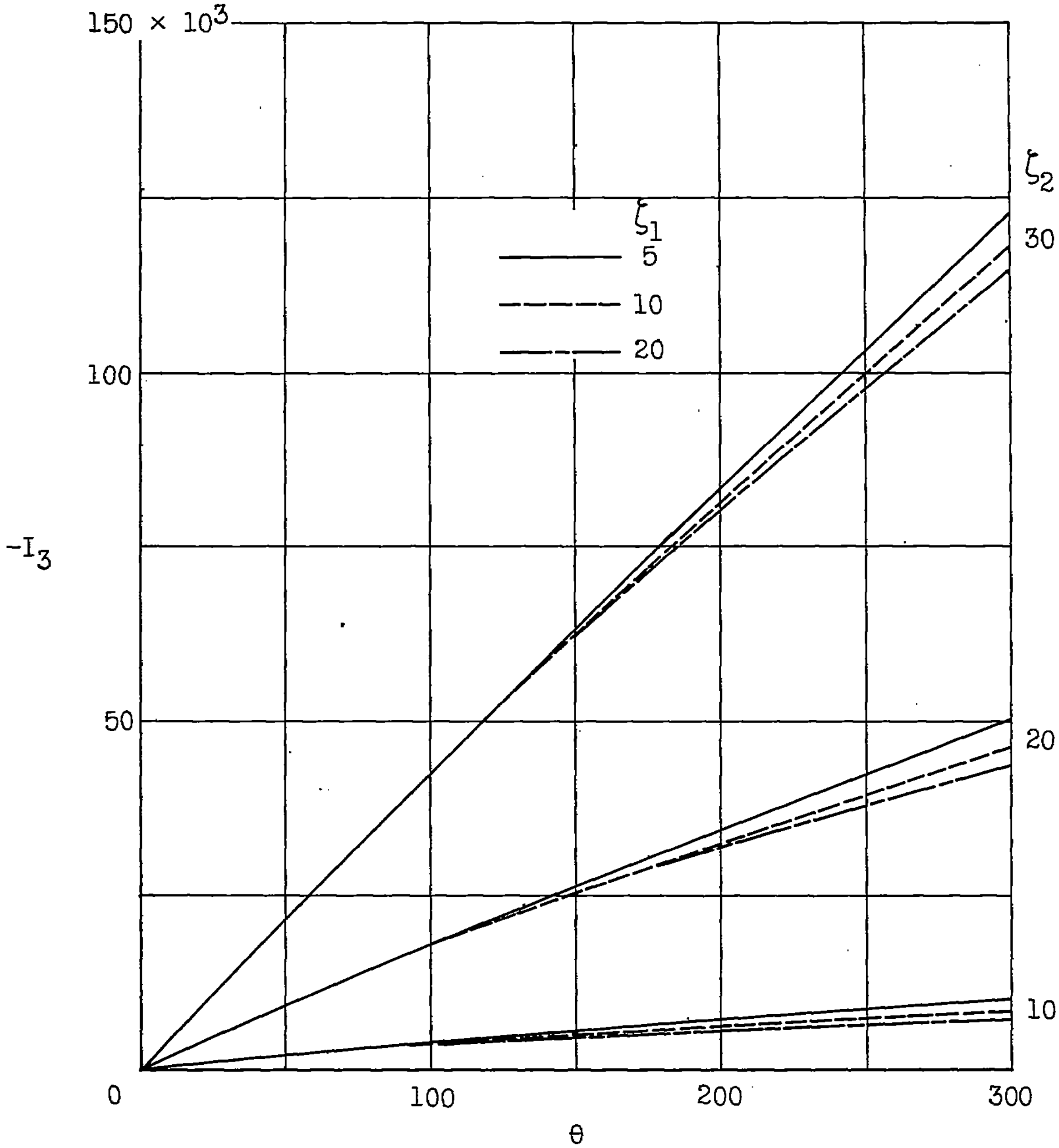

(a) $\frac{t_2}{t_1} = 1.$

Figure 20.- Values of function I_3 appearing in stress equations for angle and channel sections.

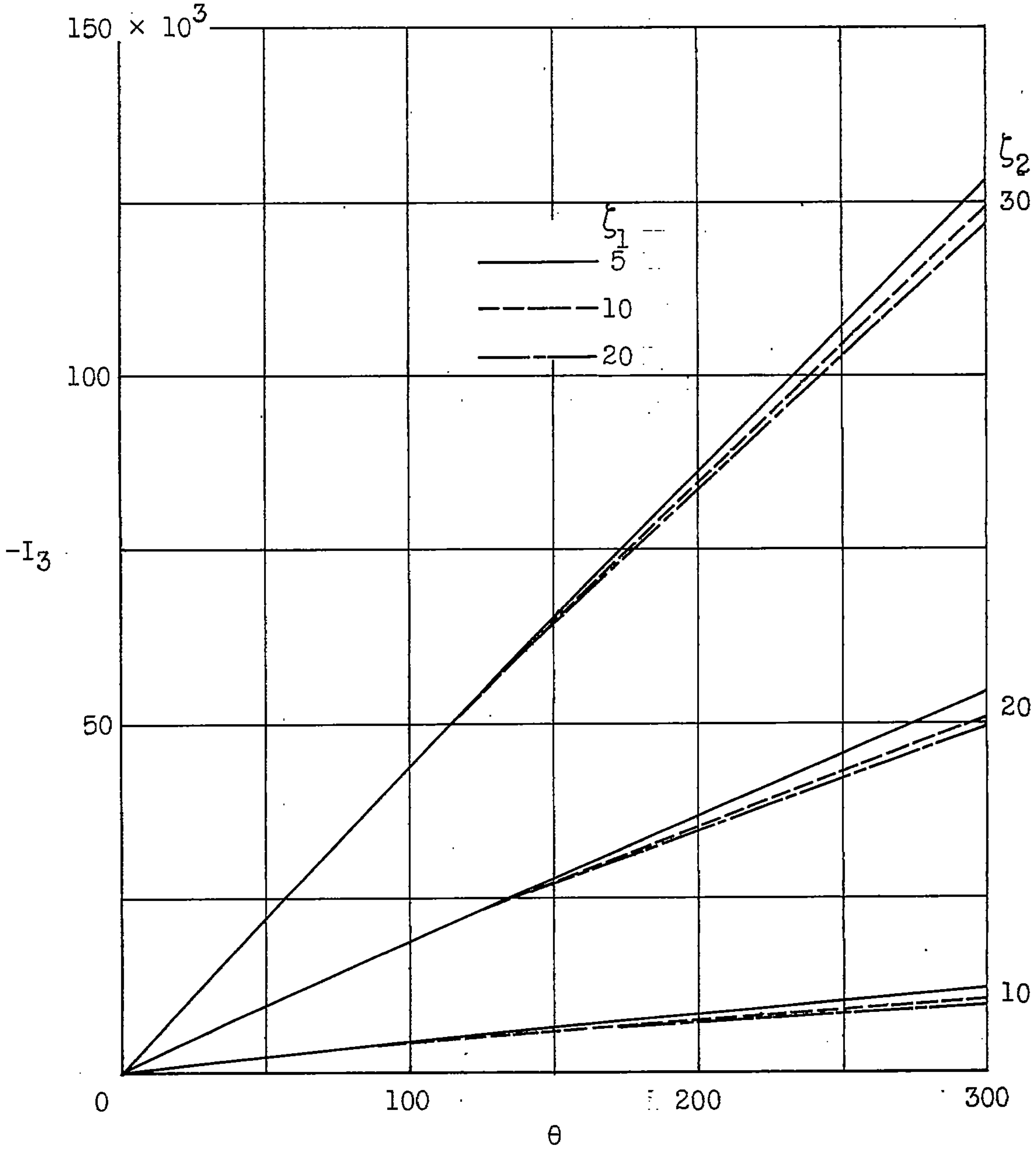

(b) $\frac{t_2}{t_1} = 2.$

Figure 20.- Continued.

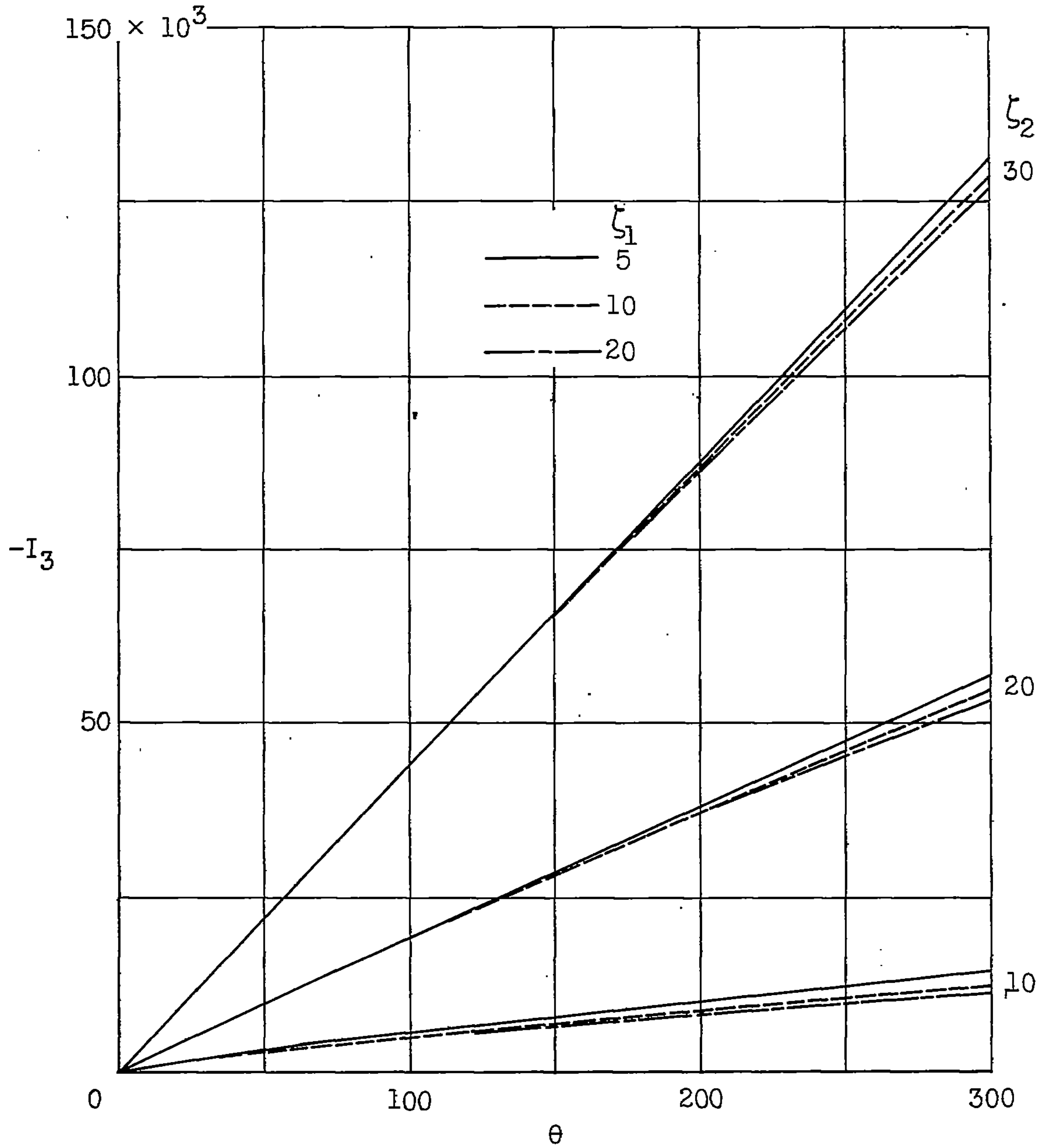

(c) $\frac{t_2}{t_1} = 4.$

Figure 20.- Concluded.

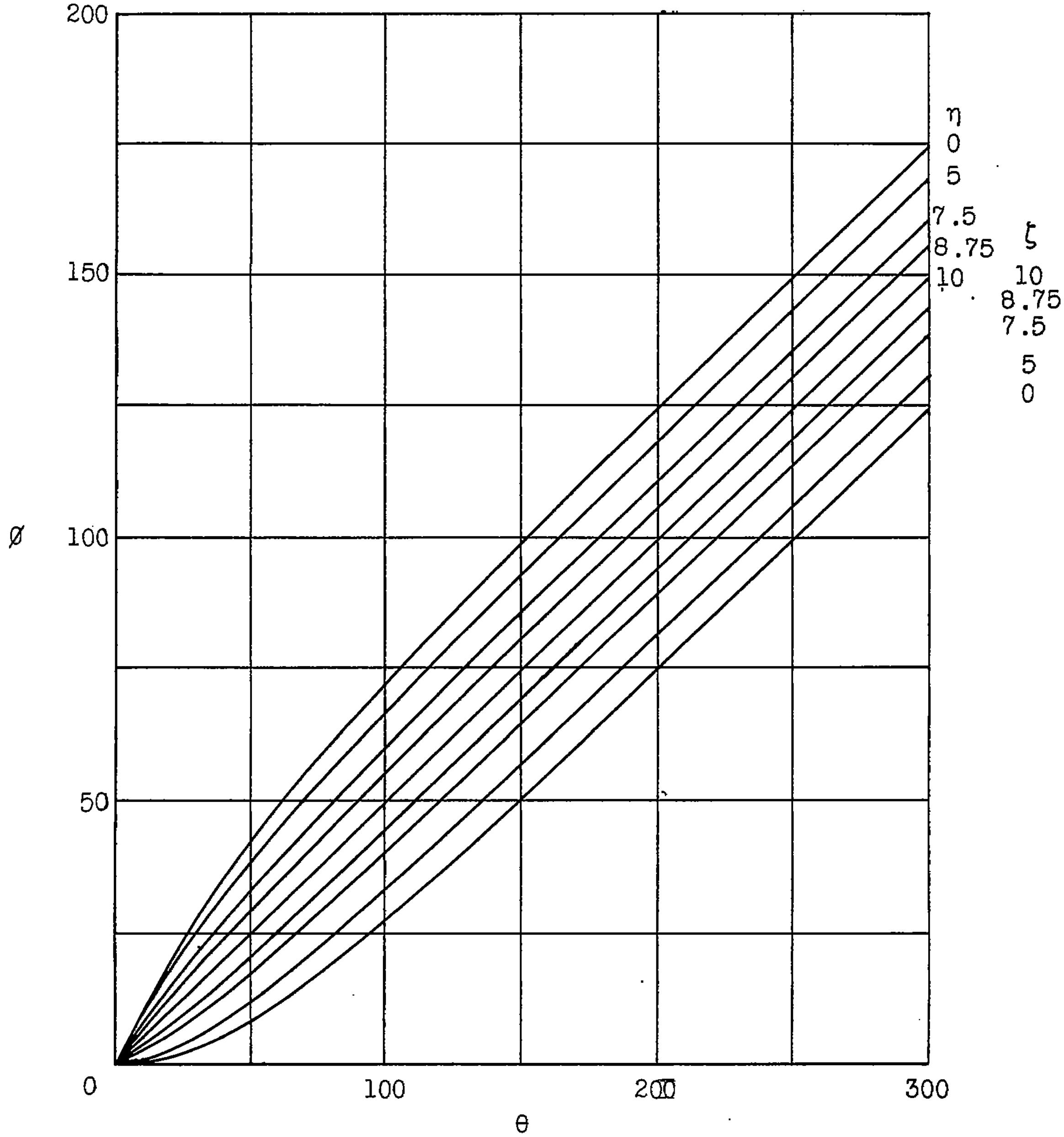

Figure 21.- Temperature history of example angle section.

$$\frac{t_2}{t_1} = 1; \ \zeta_1 = \zeta_2 = 10.$$

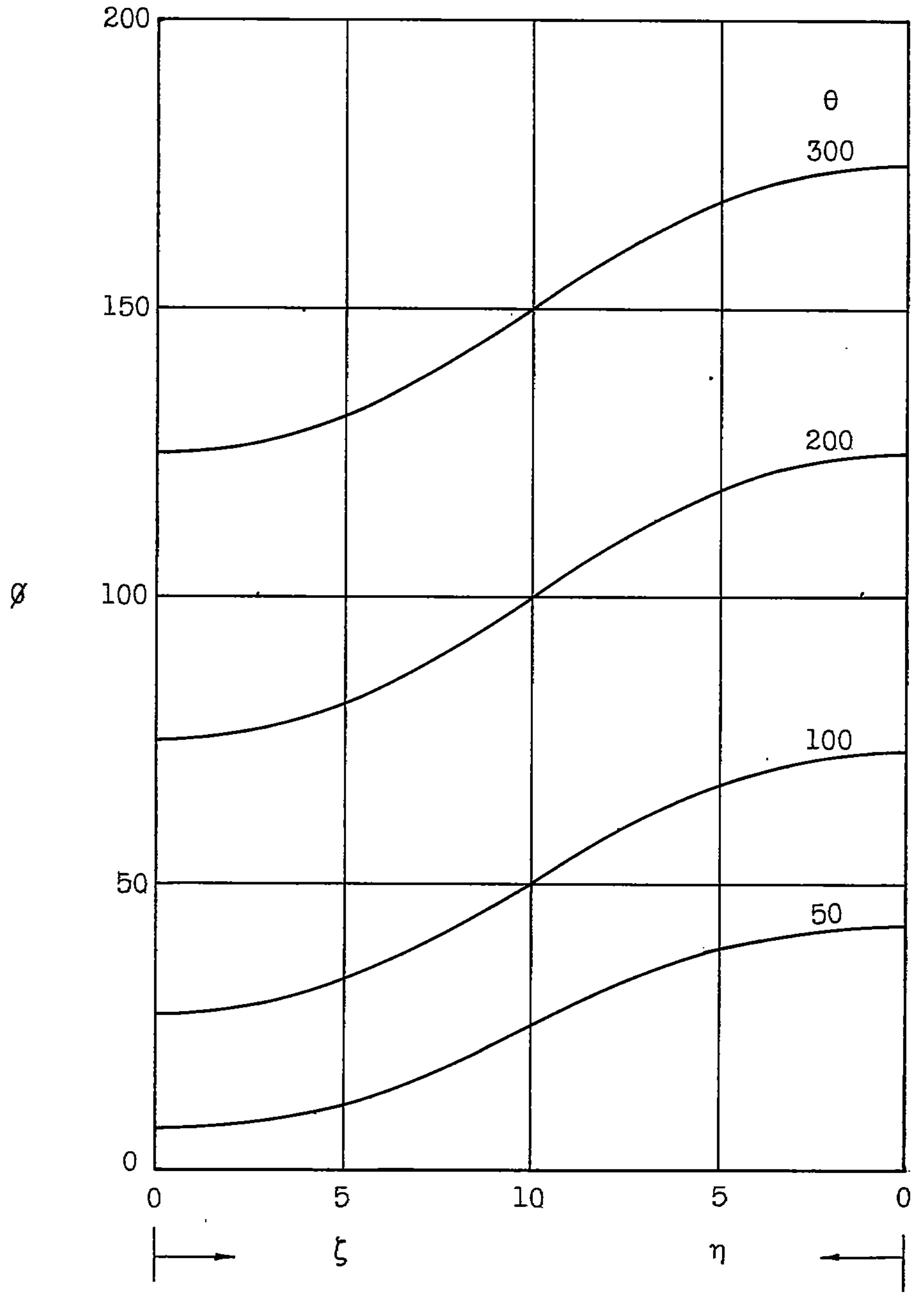

Figure 22.- Temperature distribution in example angle section.

$$\frac{t_2}{t_1} = 1; \; \zeta_1 = \zeta_2 = 10.$$

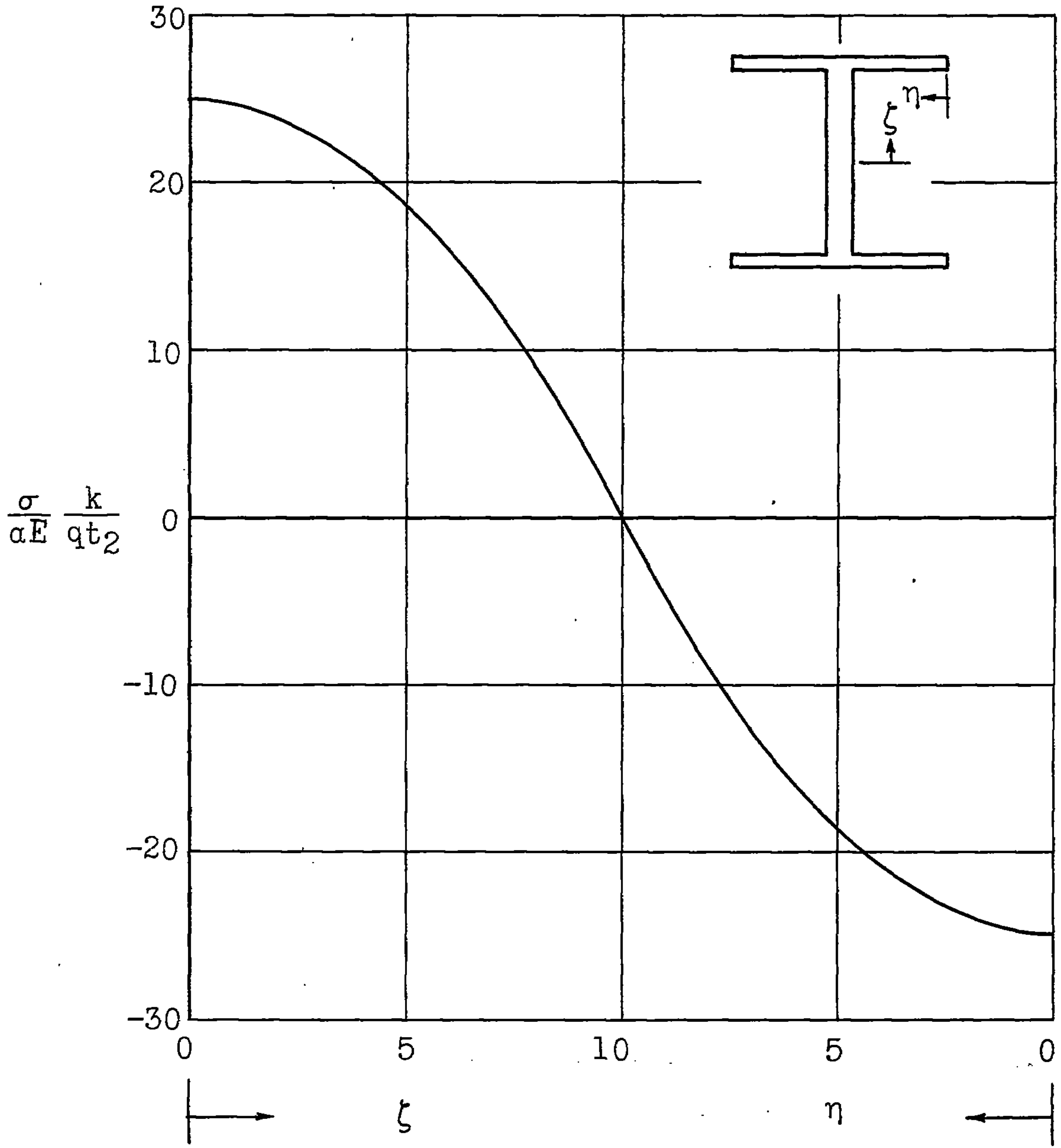

(a) H-section.

Figure 23.- Distribution of steady-state thermal stresses in structural shapes composed of angle sections. $\frac{t_2}{t_1} = 1$; $\zeta_1 = \zeta_2 = 10$.

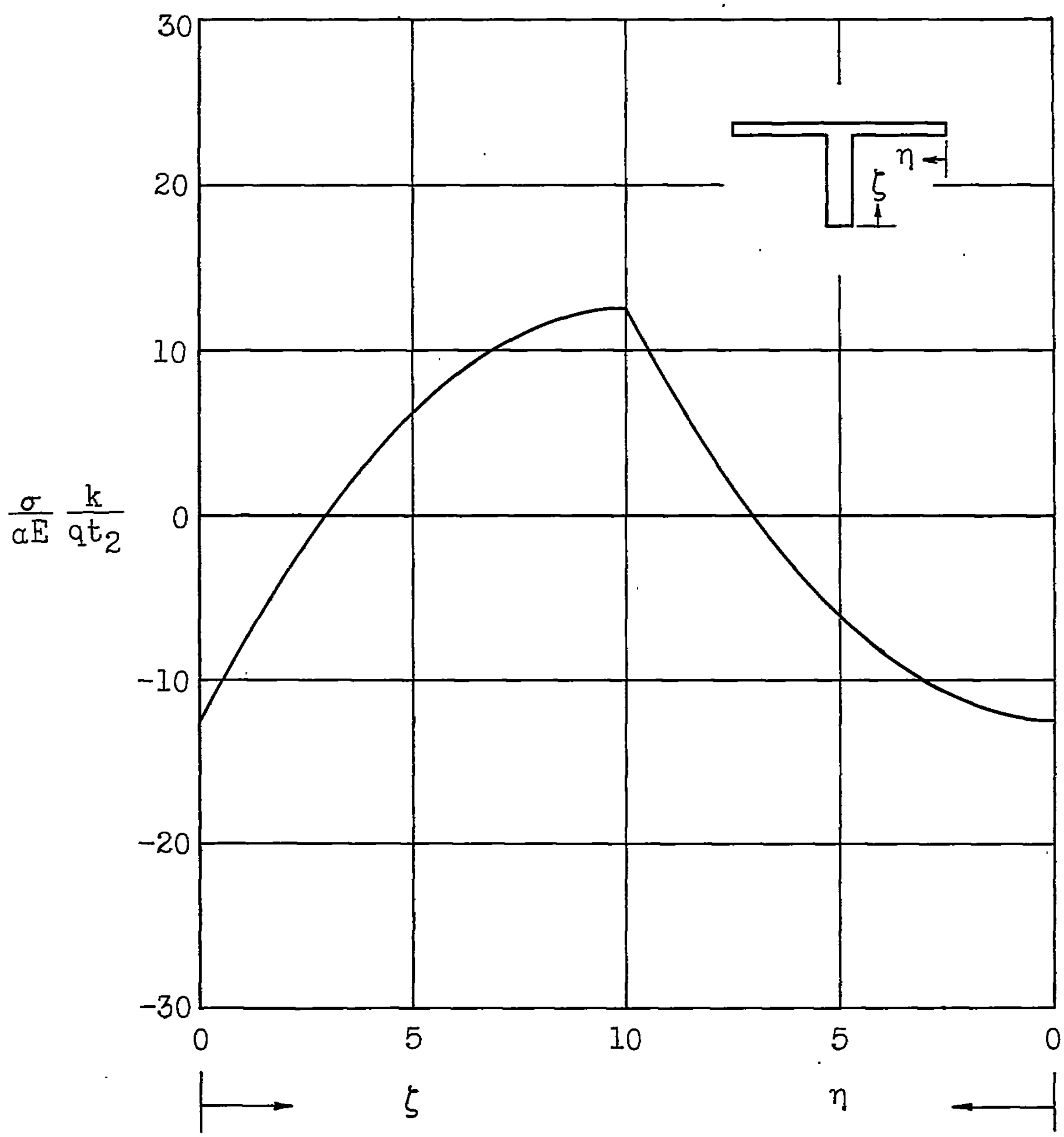

(b) T-section.

Figure 23.- Continued.

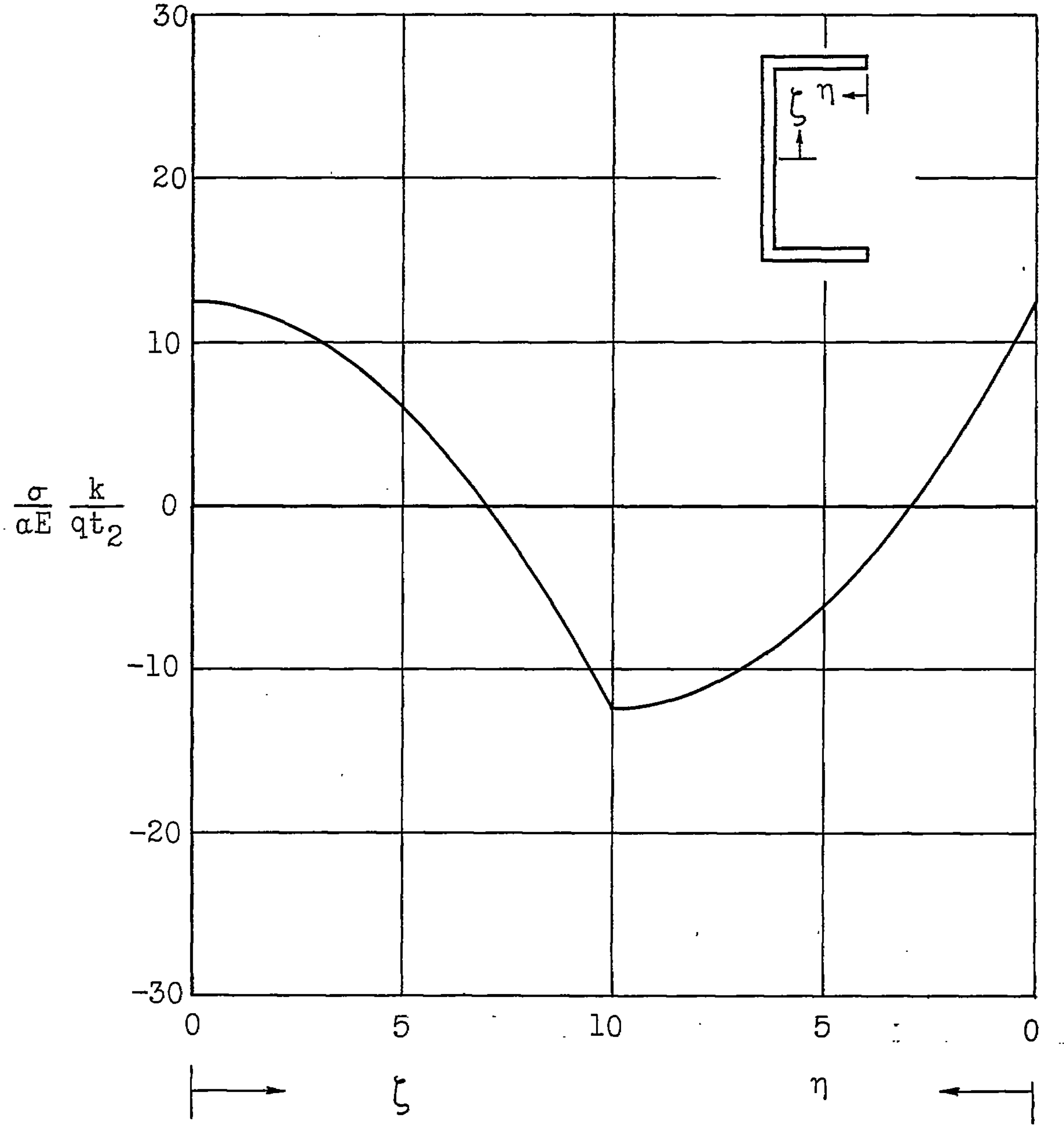

(c) Channel section.

Figure 23.- Continued.

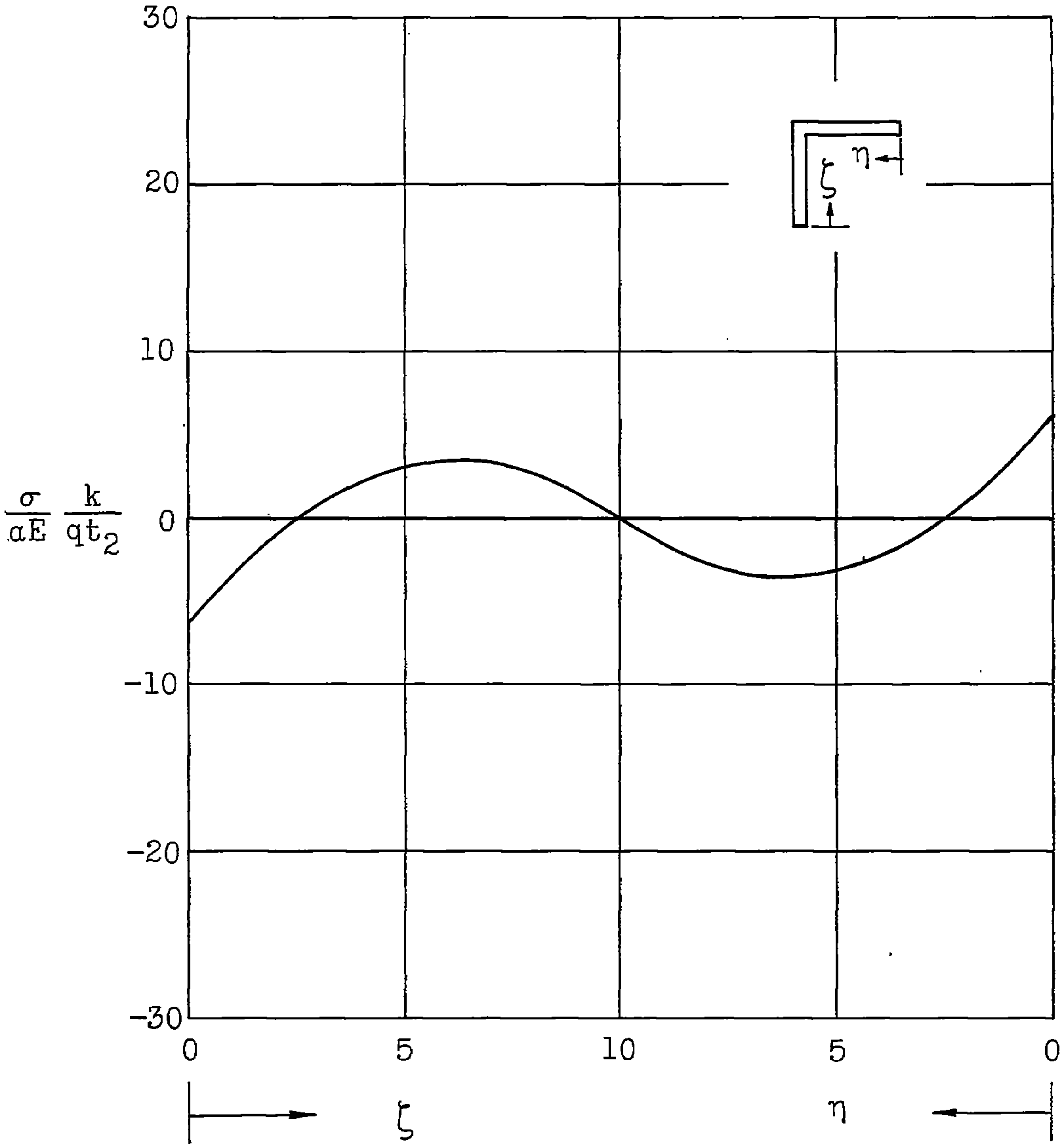

(d) Angle section.

Figure 23.- Concluded.